Exploring Structured Semantic Priors Underlying Diffusion Score for Test-time Adaptation

Mingjia Li

Beijing Institute of Technology mingjiali@bit.edu.cn

Shuang Li*

Beihang University shuangliai@buaa.edu.cn

Tongrui Su

Beijing Institute of Technology molarsu@bit.edu.cn

Longhui Yuan

Beijing Institute of Technology longhuiyuan@bit.edu.cn

Jian Liang

Kuaishou Technology liangjian03@kuaishou.com

Wei Li*

Inceptio Technology liweimcc@gmail.com

Abstract

Capitalizing on the complementary advantages of generative and discriminative models has always been a compelling vision in machine learning, backed by a growing body of research. This work discloses the hidden semantic structure within score-based generative models, unveiling their potential as effective discriminative priors. Inspired by our theoretical findings, we propose DUSA to exploit the structured semantic priors underlying diffusion score to facilitate the test-time adaptation of image classifiers or dense predictors. Notably, DUSA extracts knowledge from a single timestep of denoising diffusion, lifting the curse of Monte Carlo-based likelihood estimation over timesteps. We demonstrate the efficacy of our DUSA in adapting a wide variety of competitive pre-trained discriminative models on diverse test-time scenarios. Additionally, a thorough ablation study is conducted to dissect the pivotal elements in DUSA. Code is publicly available at https://github.com/BIT-DA/DUSA.

1 Introduction

The combination of generative and discriminative modeling has always been appealing due to their distinct nature in data comprehension [1, 2, 3, 4]. Discriminative models are adept at making accurate predictions on training data [5, 6, 7, 8, 9, 10, 11], but can be fragile when confronted with unseen data [12]. This vulnerability can be attributed to their tendency to learn spurious correlation as a shortcut, hindering their transferability [13]. Generative models, however, are proficient in capturing the underlying structure of the data, giving them an edge in grasping the whole picture [14, 15, 16] and enhancing robustness [17, 18]. Prior works have verified the effectiveness of generative objectives in discriminative learning [4, 19], yet the utilization of pre-trained generative models is under-explored.

The recent surge of diffusion models [20, 21, 22] has ignited interest in adopting them for applications beyond image generation [23, 24, 25, 26]. In the context of test-time adaptation, a pre-trained task model is updated on the fly to make accurate predictions on incoming target samples without access to their labels. This presents challenges, as the target data distribution may differ from that encountered during pre-training. The literature reveals that we can not only extract discriminative features from capacious diffusion models [23, 24, 26, 27, 28], but also convert these models into generative classifiers that demonstrate human-level generalization on out-of-distribution samples [25, 29, 30]. Such properties render them viable choices for facilitating the test-time adaptation of discriminative models, which may underperform on unseen data [31]. Diffusion-TTA [32] ranks among the first

38th Conference on Neural Information Processing Systems (NeurIPS 2024).

^{*}Corresponding author.

to employ diffusion models for test-time adaptation, where task outputs are used to modulate the conditioning of a diffusion model with the objective of likelihood maximization. While Diffusion-TTA is competitive, there's still room to unleash the full potential of diffusion models. To achieve this, two key aspects warrant further exploration. First, the conditioning space is typically low-dimensional in diffusion models [20, 22], which restricts its ability to capture the intricacies of complex data and thus impedes its expressiveness as a discriminative prior. Further, the common image-level condition lacks a fine-grained connection with data, limiting its potential in guiding dense prediction tasks. Conversely, the high-dimensional latent space of diffusion models exhibits a surprisingly interpretable semantic structure [33, 34, 35, 36, 37], making it a good fit for assisting discriminative tasks and easily extensible to dense prediction. Second, Diffusion-TTA is heavily reliant on the Monte Carlo method over as many as 180 timesteps to estimate a biased approximation of likelihood [32, 38], resulting in high computational complexity proportional to sampled timesteps.

With this work, we aim to boost test-time adaptation performance by digging into the semantic structure of diffusion models in the latent space, while lifting reliance on the Monte Carlo sampling of timesteps. Although a few works elucidate the semantic properties of the latent space [34, 37], they all take a generative viewpoint and are not tailored for discriminative tasks. We instead depart from the perspective of score functions [39, 40, 41] on the latent space, which is closely related to the denoising diffusion formulation [38, 42, 43]. Our method features exploring the structured semantic priors underlying **D**iff**U**sion models as **S**core estimators for test-time **A**daptation (**DUSA**).

Concretely, we start by providing a theoretical illustration of the semantic structure underneath the score functions $\nabla_{\mathbf{x}} \log p(\mathbf{x} \mid y)$, where the conditional probability $p(y \mid \mathbf{x})$ is implicitly embedded. The theoretical findings not only unveil discriminative priors hidden within score-based diffusion models, but applies to every single timestep and avoids likelihood estimation. A test-time objective is then derived by substituting the pre-trained task model and diffusion model for the implicit priors and score functions, respectively. Intuitively, the precise score estimation by diffusion models forms a well-structured semantic space, where the task model can learn implicit discriminative priors. Given their generative nature, the priors are further blessed with improved robustness, ultimately benefiting task prediction. Another key advantage of our approach lies in shifting computational complexity from timesteps to the number of classes, which aligns closely with our focus on discriminative tasks. Thereby, a more efficient adaptation scheme can be enabled through our practical designs.

Besides, the capacity of our DUSA is testified across a variety of task model families, test-time adaptation protocols, and task categories. Our DUSA consistently outperforms the competitive counterparts in adapting pre-trained classifiers with different backbones to out-of-distribution scenarios, whether in the mild protocol of data from a single domain [44] or the more challenging one with a continually changing datastream [45]. We also showcase the versatility of our DUSA by applying it almost as-is to test-time semantic segmentation. All diffusion models employed are trained on the corresponding source domain of the task model. Extensive analyses of the components in our method back the validity of DUSA and underline the benefits of borrowing knowledge from generative modeling.

Our main contributions can be summarized as:

- A novel proposition is given from a theoretical perspective to extract discriminative priors from score-based diffusion models, which are single-timestep-based and versatile enough to handle both classification and dense prediction tasks at test time.
- Inspired by the proposition and enhanced by practical designs, our DUSA effectively leverages
 the structured semantic priors and rivals in test-time adaptation with improved efficiency.
- DUSA outperforms the best existing methods by +5.1% and +7.3% in fully and continual test-time adaptation on ConvNeXt-L and +4.2% in test-time semantic segmentation on SegFormer-B5, validating the excellence of our method in extracting valuable priors from diffusion models.

2 Preliminaries

Test-time adaptation. A model well-trained on source data can face severe performance degradation on out-of-distribution (OOD) target samples. To tackle this, test-time adaptation (TTA) [44] is proposed to boost model performance at inference time. Formally, an off-the-shelf model $f_{\theta}(\mathbf{x})$ pre-trained on labeled source data $\mathcal{D}_{\mathcal{S}} = \{(\mathbf{x}_i, y_i)\}_{i=1}^N$ is adopted as the task model, where the source data follows a probability distribution $\mathbf{x}_i \sim P_{\mathcal{S}}(\mathbf{x})$ and is inaccessible during adaptation. TTA aims

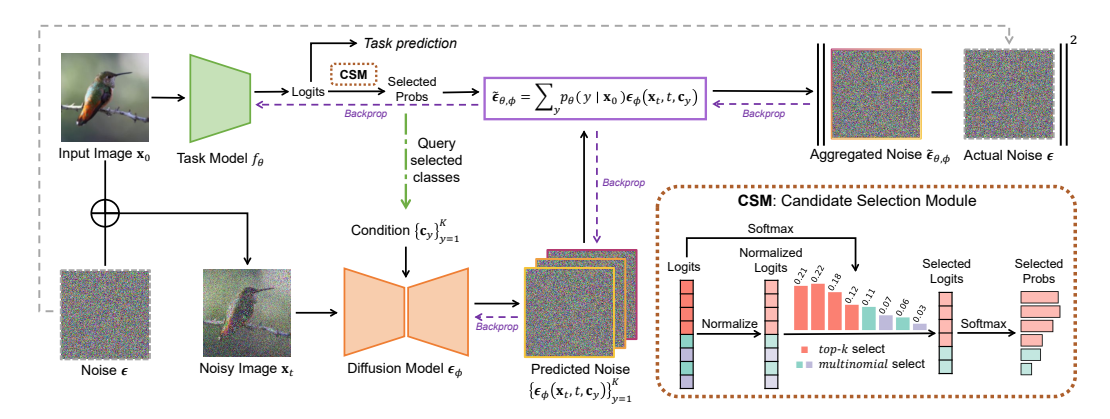


Figure 1: **Overview of DUSA**. Our method adapts a discriminative task model f_{θ} with a generative diffusion model ϵ_{ϕ} . Given image \mathbf{x}_0 at test-time, the task model outputs logits. To improve efficiency, we devise a CSM to select classes to adapt and return their probabilities (probs). The embeddings of the classes are then queried as diffusion model conditions, yielding conditional noise predictions from noisy image \mathbf{x}_t . The aggregated noise $\tilde{\epsilon}_{\theta,\phi}$ is then constructed from ensembling conditional noises with probs, which is aligned with the added noise ϵ following Eq. (10). Both models are updated.

at pushing the limits of model performance on unlabeled target data $\mathcal{D}_{\mathcal{T}} = \{\mathbf{x}_j\}_{j=1}^M$ on the fly, where the target data follows $\mathbf{x}_j \sim P_{\mathcal{T}}(\mathbf{x})$ and $P_{\mathcal{S}}(\mathbf{x}) \neq P_{\mathcal{T}}(\mathbf{x})$. With batched target data arriving online, we obtain predictions from the task model $f_{\theta}(\mathbf{x})$ and update it on live target samples without labels.

Diffusion models. Diffusion models excel at modeling data distribution $p(\mathbf{x})$ by learning to restore the gradually destroyed data structure [20, 38, 46]. For diffusion models, a forward and a reverse process is defined. In the forward process, small Gaussian noise is iteratively applied to real data \mathbf{x}_0 :

$$q(\mathbf{x}_t \mid \mathbf{x}_{t-1}) := \mathcal{N}(\mathbf{x}_t; \sqrt{1 - \beta_t} \mathbf{x}_{t-1}, \beta_t \mathbf{I}), \tag{1}$$

where $\{\beta_t \in (0,1)\}_{t=1}^T$ is a variance schedule defining the noise added at each timestep t.

With the reparameterization trick, the noisy version of x_0 can be directly obtained in a single step:

$$\mathbf{x}_t = \sqrt{\bar{\alpha}_t} \mathbf{x}_0 + \sqrt{1 - \bar{\alpha}_t} \boldsymbol{\epsilon}, \ \boldsymbol{\epsilon} \sim \mathcal{N}(\mathbf{0}, \mathbf{I}),$$
 (2)

where $\alpha_t \coloneqq 1 - \beta_t$, $\bar{\alpha}_t \coloneqq \prod_{i=1}^t \alpha_i$, and the sampled noise ϵ is of the same dimensionality as \mathbf{x}_0 .

In the reverse process, a conditional diffusion model [20, 21, 22, 47, 48] $\epsilon_{\phi}(\mathbf{x}_t, t, \mathbf{c})$ is trained to predict the noise added to \mathbf{x}_t with condition \mathbf{c} , by minimizing the simplified denoising objective:

$$\mathcal{L}_{simple}(\phi) := \mathbb{E}_{(\mathbf{x}_0, \mathbf{c}), \epsilon, t} [\|\epsilon - \epsilon_{\phi}(\mathbf{x}_t, t, \mathbf{c})\|_2^2].$$
(3)

3 Structured Semantic Priors in Diffusion Score for Test-Time Adaptation

In this section, we first review a relevant method (Sec. 3.1), then provide the theoretical insight behind our DUSA (Sec. 3.2). At last, we advocate a few practical designs with efficiency in mind (Sec. 3.3). The framework of our DUSA is illustrated in Fig. 1. Given a pre-trained task model, a set of classes to optimize is selected by the Candidate Selection Module (CSM) based on task model prediction to improve adaptation efficiency. We focus on the selected classes and aggregate the conditional noise estimations with CSM-modulated probabilities on these classes, upon which our DUSA objective is constructed. The structured semantic priors of the diffusion model are then propagated to the task model through our objective. For more details please refer to Alg. 1 in Appendix E.

3.1 A Brief Review of Diffusion-TTA

Diffusion-TTA [32] takes the first step in exploring conditional diffusion models for test-time adaptation. In Diffusion-TTA, the task model prediction $p_{\theta}(y \mid \mathbf{x}_0)$ is integrated with class embeddings

 $\{\mathbf{c}_y\}_{y=1}^N$ to get a soft condition $\mathbf{c} = \sum_y p_\theta(y \mid \mathbf{x}_0) \mathbf{c}_y$, where N is the number of classes. The samplewise adaptation is performed with the diffusion loss: $\mathcal{L}(\theta, \phi) = \mathbb{E}_{t, \epsilon}[\|\epsilon - \epsilon_{\phi}(\mathbf{x}_t, t, \mathbf{c})\|_2^2]$. Inspired by [25], the loss is averaged over hundreds of (t, ϵ) pairs to remedy the performance degradation caused by incorrect class prediction using a single timestep [32], at the cost of reduced efficiency.

3.2 Unlocking the Discriminative Power of Conditional Diffusion Models

Unlike previous attempts that rely heavily on a massive number of timesteps to provide an appropriate estimation of likelihood $p(\mathbf{x} \mid \mathbf{c})$ [25, 29, 32], we shed light on the semantic structure underneath the denoising capability of conditional diffusion models from the perspective of score functions [39, 40, 41, 42], which will be shown to hold for every single timestep. Proofs can be found in Appendix C.

We first present our main theoretical contribution to reveal the semantic structure of score functions: **Proposition 1.** Let $p(\mathbf{x})$ and $\{p(\mathbf{x} \mid y) : y \in \mathcal{Y}\}$ be continuously differentiable probability densities, their score functions $\nabla_{\mathbf{x}} \log p(\mathbf{x})$ and $\{\nabla_{\mathbf{x}} \log p(\mathbf{x} \mid y) : y \in \mathcal{Y}\}$, the following equation holds:

$$\nabla_{\mathbf{x}} \log p(\mathbf{x}) = \sum_{y} p(y \mid \mathbf{x}) \nabla_{\mathbf{x}} \log p(\mathbf{x} \mid y). \tag{4}$$

Remark. The equation holds under mild assumptions about the densities but applies to any data xwith an entire set of conditions $\{y:y\in\mathcal{Y}\}$. All score functions can be estimated by score matching or denoising diffusion. Note that the posteriors $\{p(y \mid \mathbf{x}) : y \in \mathcal{Y}\}\$ are **not** directly modeled, and thus can be seen as the **implicit priors** hidden in the construction of (conditional) score functions.

To link our Proposition 1 with a trained diffusion model, we revisit Tweedie's Formula [49], which serves as a key connection between score functions and the formulation of diffusion models [43]:

Lemma 1 (Tweedie's Formula). Let $\mathbf{z} \mid \boldsymbol{\mu}_{\mathbf{z}} \sim \mathcal{N}(\mathbf{z}; \boldsymbol{\mu}_{\mathbf{z}}, \boldsymbol{\Sigma}_{\mathbf{z}})$, then the posterior expectation of $\boldsymbol{\mu}_{\mathbf{z}}$ given **z** can be estimated by:

$$\mathbb{E}[\boldsymbol{\mu}_{\mathbf{z}} \mid \mathbf{z}] = \mathbf{z} + \boldsymbol{\Sigma}_{\mathbf{z}} \nabla_{\mathbf{z}} \log p(\mathbf{z}). \tag{5}$$

As Eq. (2) indicates $q(\mathbf{x}_t \mid \mathbf{x}_0) = \mathcal{N}(\mathbf{x}_t; \sqrt{\bar{\alpha}_t}\mathbf{x}_0, (1 - \bar{\alpha}_t)\mathbf{I})$, we have the following corollary: **Corollary 1.** Let $\epsilon \sim \mathcal{N}(\mathbf{0}, \mathbf{I})$ be a sampled noise in a forward process parameterized by $\{\bar{\alpha}_t\}_{t=1}^T$ to get noisy data \mathbf{x}_t , the connection between score function $\nabla_{\mathbf{x}_t} \log p(\mathbf{x}_t)$ and noise ϵ can be given by: $\nabla_{\mathbf{x}_t} \log p(\mathbf{x}_t) = -\frac{\epsilon}{\sqrt{1-\bar{\alpha}_t}}.$ (6)

$$\nabla_{\mathbf{x}_t} \log p(\mathbf{x}_t) = -\frac{\epsilon}{\sqrt{1 - \bar{\alpha}_t}}.$$
 (6)

Recall that our Proposition 1 makes no assumptions on the form of data x, thus it holds for the noisy data \mathbf{x}_t at any single timestep t. Applying Eq. (6) to Eq. (4) at timestep t, we get the following:

$$-\frac{\epsilon}{\sqrt{1-\bar{\alpha}_t}} = \sum_{y} p(y \mid \mathbf{x}_t) \nabla_{\mathbf{x}_t} \log p(\mathbf{x}_t \mid y).$$
 (7)

For diffusion models, the conditional score function $\nabla_{\mathbf{x}_t} \log p(\mathbf{x}_t \mid y)$ can be estimated as follows:

$$\nabla_{\mathbf{x}_t} \log p(\mathbf{x}_t \mid y) \approx -\frac{\epsilon_{\phi}(\mathbf{x}_t, t, \mathbf{c}_y)}{\sqrt{1 - \bar{\alpha}_t}},$$
(8)

and therefore we can combine Eq. (7) and Eq. (8) to give a structured estimation in the latent space:

$$\epsilon \approx \sum_{y} p(y \mid \mathbf{x}_t) \epsilon_{\phi}(\mathbf{x}_t, t, \mathbf{c}_y),$$
 (9)

where all score functions are now replaced by noise predictors. Note that $p(y \mid \mathbf{x}_t)$ is the implicit prior of a conditional diffusion model at a single timestep t, and thus can be learned by directly plugging the task model prediction on \mathbf{x}_0 , dubbed as $p_{\theta}(y \mid \mathbf{x}_0)$, into Eq. (9). The objective to minimize is:

$$\mathcal{L}_{DUSA}(\theta, \phi) = \mathbb{E}_{\epsilon} \Big[\| \epsilon - \sum_{y} p_{\theta}(y \mid \mathbf{x}_{0}) \epsilon_{\phi}(\mathbf{x}_{t}, t, \mathbf{c}_{y}) \|_{2}^{2} \Big].$$
 (10)

Intuitively, the optimization of this objective encourages the task model to extract knowledge from the semantic structure of a capacious diffusion model, promising better robustness for adaptation.

Corollary 2. The objective in Eq. (10) is extensive to \mathbf{x}_0 -prediction or \mathbf{v} -prediction [50] in diffusion.

With a total of K classes and T timesteps and computational burden primarily borne by diffusion models, our DUSA shows a task-relevant time complexity of $\mathcal{O}(K)$, while that of Diffusion-TTA is the diffusion-relevant $\mathcal{O}(T)$. Enhanced by practical designs in Sec. 3.3, we empirically find that our DUSA establishes leading performance even with a small budget, leaving Diffusion-TTA behind.

Free lunch in modern diffusion models. The proposed objective in Eq. (10) requires the joint training of task model $f_{\theta}(\mathbf{x})$ and diffusion model $\epsilon_{\phi}(\mathbf{x}_t, t, \mathbf{c}_y)$ over all conditions $\{\mathbf{c}_y : y \in \mathcal{Y}\}$ simutaneously. The training inefficiency largely stems from the excessive adaptation of the diffusion model, which may not always require knowledge from the task model.

Indeed, Eq. (10) can be interpreted from two distinct perspectives. From one viewpoint, the task model extracts knowledge from the implicit priors of the diffusion model. From another, a weighted optimization is applied to conditional noise estimations, allowing the diffusion model to adapt to the incoming test-time data based on task model predictions. Alternatively, the adaptation of diffusion models can be achieved by introducing unconditional noise estimations with null condition \varnothing :

$$\epsilon \approx \epsilon_{\phi}(\mathbf{x}_t, t, \varnothing).$$
 (11)

Combining Eq. (9) and Eq. (11) reveals another semantic structure within the diffusion model:

$$\epsilon_{\phi}(\mathbf{x}_t, t, \varnothing) \approx \sum_{y} p(y \mid \mathbf{x}_t) \epsilon_{\phi}(\mathbf{x}_t, t, \mathbf{c}_y),$$
 (12)

where $\epsilon_{\phi}(\mathbf{x}_t,t,\varnothing)$ and $\{\epsilon_{\phi}(\mathbf{x}_t,t,\mathbf{c}_y):y\in\mathcal{Y}\}$ represent noise estimations from a specific diffusion model capable of handling both unconditional and conditional generation. Note that the implicit priors $\{p(y\mid\mathbf{x}_t):y\in\mathcal{Y}\}$ in Eq. (12) serve as a critical link between the unconditional and conditional noise estimations. Therefore, an unconditional adaptation of the diffusion model implicitly facilitates its conditional adaptation to the test-time scenario, without reliance on the task model.

Modern conditional diffusion models [20, 22] maintain their unconditional generation capability by employing an additional null condition that replaces the original class conditions with a certain probability (typically 10%). Leveraging this feature, we can adjust the objective to enhance efficiency:

$$\mathcal{L}_{cond}(\theta) = \mathbb{E}_{\epsilon} \Big[\| \epsilon - \sum_{y} p_{\theta}(y \mid \mathbf{x}_{0}) \epsilon_{\phi}(\mathbf{x}_{t}, t, \mathbf{c}_{y}) \|_{2}^{2} \Big], \quad \mathcal{L}_{uncond}(\phi) = \mathbb{E}_{\epsilon} \Big[\| \epsilon - \epsilon_{\phi}(\mathbf{x}_{t}, t, \emptyset) \|_{2}^{2} \Big],$$

$$\mathcal{L}_{DUSA-U}(\theta, \phi) = \mathcal{L}_{cond}(\theta) + \mathcal{L}_{uncond}(\phi),$$
(13)

where the diffusion model is now unconditionally adapted. An immediate concern is whether such modifications would impact adaptation performance. We empirically find it can significantly boost training efficiency with minor to no performance degradation, please refer to Sec. 4.1 for more details.

Readily applicable to dense prediction tasks. It is worth noting that our method is not confined to classification tasks, but can be easily applied to a handful of dense prediction tasks as well. Taking semantic segmentation as an example, the task model $p_{\theta}(\mathbf{y} \mid \mathbf{x}_0)$ is now a dense labeler assigning per-pixel class labels to the input, where \mathbf{y} is the predicted segmentation map of shape $H \times W \times K$, $H \times W$ is the size of input image \mathbf{x}_0 , and K is the number of interested classes. Again, our proposition is nowhere strict on the form of data, and therefore should be readily applicable to every single pixel in \mathbf{x}_0 . The new objective to minimize is then easily obtained by utilizing Eq. (4) in a per-pixel fashion:

$$\mathcal{L}_{DUSA\text{-}seg}(\theta, \phi) = \mathbb{E}_{\boldsymbol{\epsilon}, (h, w)} \Big[\| \boldsymbol{\epsilon} - \sum_{k=1}^{K} p_{\theta}(\mathbf{y} \mid \mathbf{x}_{0})_{h, w, k} \cdot \boldsymbol{\epsilon}_{\phi}(\mathbf{x}_{t}, t, \mathbf{c}_{k})_{h, w} \|_{2}^{2} \Big], \tag{14}$$

where (h, w) denotes the pixel location in an image sample of size $H \times W$, and \mathbf{c}_k represents the class embedding of a class k in the segmentation task. We highlight that per-pixel noise can be efficiently acquired by extracting elements from the image-level noise estimation $\epsilon_{\phi}(\mathbf{x}_t, t, \mathbf{c}_k)$, which takes the entire data sample \mathbf{x}_t and class-wise condition \mathbf{c}_k as inputs. As a vast majority of diffusion models are trained with image-level annotations, this design is advantageous as it allows the use of off-the-shelf diffusion models without modifying their training schemes. In contrast, Diffusion-TTA [32] requires the integration of per-pixel conditions into diffusion models to accommodate dense prediction tasks.

3.3 Improving Adaptation Efficiency with Practical Designs

Identifying appropriate timestep. Since our DUSA intends to extract structured semantic priors from a single timestep, a critical question emerges: which timestep should we utilize to maximize adaptation performance? Iterating over all T timesteps for a certain task model on a specific task is just not practical, and thus a universal preference must be advocated. While the semantic structure uncovered in Eq. (4) is valid for all timesteps in theory, the estimation of score functions by denoising diffusion models [20, 22] can be unreliable. As pointed out by [51, 52], for diffusion models we have

a scheduled $\bar{\alpha}_t$ decreasing with t and $\bar{\alpha}_t \to 1$ when $t \to 0$, which directly amplifies error in score estimation by Eq. (9) at smaller timesteps. A large timestep is also not recommended, as denoising at higher noise levels is more challenging [38], posing a greater challenge to score estimation. Based on the preceding conclusions, we select timestep t=100 and find it suits well for all our experiments.

Utilizing task model for candidate selection. Similar to Diffusion Classifiers [25, 29], our DUSA has a computational complexity that scales proportional to class number. To circumvent the slowdown by a large number of classes, we utilize task model prediction to significantly improve adaptation efficiency. With the observation that classifiers typically maintain a top-k accuracy [53] and top-k accuracy is our main concern in the test-time adaptation of discriminative models, we opt to apply our DUSA to the most promising classes. Specifically, we deem the posterior $p(y \mid \mathbf{x})$ of less likely class candidates to be zero and only optimize the semantic structure among the selected classes.

A mere decrease in class number can lead to optimization issues, as the task model can be biased towards certain classes, especially with a small batch size. This can be blamed on the underutilization of the semantic structure, further exacerbated by the erratic task model prediction on the pruned classes due to a lack of constraints. To tackle this, we devise a Candidate Selection Module (CSM). In the module, we first adopt LogitNorm [54, 55] to force constraints on the pruned classes to stabilize training, where the logits output of the task model are ℓ_2 normalized before selection. Intuitively, we discourage the optimization in the magnitude of logits to mitigate overconfidence, especially on pruned classes. Then we handle the class bias problem by introducing randomness in selection. In detail, with a selection budget b=k+m, we split it into two parts: k for top-k classes select, and m for a multinomial selection without replacement from the remaining classes, where the sampling probabilities are calculated from the logits before normalization. We only focus on the selected b normalized logits, and apply softmax to get their probabilities for our DUSA objective. After a series of practical designs, we succeed in reducing the time complexity of DUSA from $\mathcal{O}(K)$ to $\mathcal{O}(b)$, where a small b should be valid for a large number of classes, as will be shown in Sec. 4.4.

4 Experiments

Datasets and models. Our experiments are conducted on three benchmarks: ImageNet-C [31] for fully and continual test-time classification, ADE20K [56] with corruptions defined in [31] (dubbed as ADE20K-C) for test-time semantic segmentation. All image corruptions are at the highest severity level 5. We use ResNet-50 [5], ViT-B/16 [57], ConvNeXt-L [6] pre-trained on ImageNet for ImageNet-C experiments, and SegFormer-B5 [58] pre-trained on ADE20K for ADE20K-C ones. We follow [59] and use the GN variant of ResNet-50 for stability. More details are in Appendix F.1.

Compared methods. We compare our DUSA with Tent [44], CoTTA [45], EATA [60], SAR [59], RoTTA [61], and Diffusion-TTA [32] for image classification. For semantic segmentation, we compare with BN Adapt [62, 63], Tent [44] and CoTTA [45]. More details are in Appendix F.2.

Evaluation metrics. Top-1 accuracy (Acc) is reported on each corruption type for image classification. For semantic segmentation, the mean Intersection-over-Union (mIoU) is reported. The main results of our DUSA all come with mean and standard deviation statistics over 3 independent runs.

Implementation details. The batch size is 64 for test-time classification tasks unless otherwise stated. Following [32], we use Adam optimizer [64] with a learning rate of 0.00001 for our DUSA and Diffusion-TTA. For other baselines, SGD with momentum 0.9 or Adam optimizer is used in line with the literature [44, 59, 60]. As for test-time semantic segmentation, the batch size is 1 and Adam with a learning rate of 0.00006/8 is used, following [45]. We use ImageNet [65] trained DiT [22] and ADE20K trained ControlNet [48] as diffusion models. More details are in Appendix F.3.

4.1 Fully Test-Time Adaptation of ImageNet Pre-trained Classifiers

Table 1 shows our DUSA in comparison with relevant methods under the online setting of test-time adaptation to every single corruption domain in ImageNet-C, also known as fully TTA [44]. Generally, our DUSA and Diffusion-TTA both achieve a substantial performance gain, thanks to the knowledge from a capacious generative diffusion model. Sepecifically, our DUSA yields a significant improvement of +21.9%, +23.3%, +15.7% on ResNet-50, ViT-B/16, and ConvNeXt-L over pre-trained classifiers. Besides, DUSA consistently outperforms the multi-timestep enhanced

Table 1: Fully test-time adaptation of ImageNet classifiers on ImageNet-C. The best results are in bold and runner-ups are underlined. GN/LN is short for Group/Layer normalization.

	Noise				В	lur			Wea	ather			Dig	gital		
Method	Gauss.	Shot	Impul.	Defoc.	Glass	Motion	Zoom	Snow	Frost	Fog	Brit.	Contr.	Elastic	Pixel	JPEG	Avg.
ResNet-50 (GN)	22.1	23.0	22.0	19.8	11.4	21.5	25.0	40.3	47.0	34.0	68.8	36.3	18.5	29.3	52.6	31.4
 Tent 	25.3	29.1	24.5	14.9	9.9	21.6	22.3	27.5	32.1	3.5	69.9	42.0	10.3	48.6	54.6	29.1
 CoTTA 	22.1	23.0	22.0	19.8	11.4	21.5	25.1	40.3	47.0	34.0	68.8	36.4	18.5	29.3	52.6	31.5
 EATA 	38.6	40.9	39.7	27.3	26.7	36.5	38.6	50.8	49.1	55.6	72.0	49.9	40.5	55.7	58.2	45.3
• SAR	39.6	42.4	41.0	19.8	22.9	37.1	38.7	27.3	47.4	55.1	72.4	48.8	7.2	54.9	57.4	40.8
 RoTTA 	22.8	23.8	22.5	19.7	12.0	21.8	25.2	41.3	47.5	34.6	69.2	36.8	19.2	29.9	52.9	31.9
 Diffusion-TTA 	42.0	44.6	42.4	38.3	39.5	46.9	48.2	56.5	56.3	60.0	72.6	45.6	57.9	61.4	58.0	51.3
 DUSA (Ours) 	$45.2_{\pm 0.0}$	$47.3_{\pm 0.0}$	$46.3_{\pm 0.1}$	$37.3_{\pm 0.1}$	$37.6_{\pm 0.2}$	$48.4_{\pm 0.0}$	$50.3_{\pm 0.3}$	59.1 $_{\pm 0.1}$	$55.6_{\pm 0.0}$	$63.3_{\pm 0.3}$	$73.3_{\pm 0.0}$	55.1 $_{\pm 0.0}$	$56.5_{\pm 0.3}$	$63.2_{\pm 0.1}$	$60.9_{\pm 0.2}$	53.3
• DUSA-U (Ours)	$45.0_{\pm 0.1}$	$47.1_{\pm 0.1}$	$46.1_{\pm 0.0}$	$36.8_{\pm 0.2}$	$37.7_{\pm 0.1}$	$47.9_{\pm 0.1}$	$49.5_{\pm 0.3}$	$59.0_{\pm 0.1}$	$55.4_{\pm 0.1}$	$63.0_{\pm 0.2}$	$73.1_{\pm 0.1}$	$54.3_{\pm 0.0}$	$56.4_{\pm 0.2}$	$62.9_{\pm 0.1}$	$60.5_{\pm 0.3}$	53.0
ViT-B/16 (LN)	38.3	35.4	38.1	29.5	24.2	32.8	30.5	36.4	45.0	50.4	68.3	22.5	39.4	52.7	53.5	39.8
 Tent 	53.9	54.5	54.1	44.4	47.2	53.8	6.7	4.6	61.9	65.4	72.9	54.9	58.0	65.1	64.1	50.8
 CoTTA 	38.3	35.4	38.1	29.5	24.2	32.8	30.5	36.4	45.0	50.4	68.3	22.5	39.4	52.7	53.5	39.8
 EATA 	55.4	56.3	55.3	48.9	53.4	58.6	58.2	63.5	64.1	67.5	74.3	56.5	65.7	68.5	66.6	60.9
• SAR	53.9	54.3	54.1	46.0	47.8	54.2	49.4	28.2	61.4	64.3	72.8	54.3	59.2	64.8	63.5	55.2
 RoTTA 	42.6	39.9	42.9	30.6	26.4	34.8	31.7	39.2	47.8	52.4	68.8	23.3	42.0	55.0	54.0	42.1
 Diffusion-TTA 	52.1	54.5	53.5	49.3	52.9	56.9	55.6	60.6	63.0	64.2	72.6	47.4	66.4	67.6	62.5	58.6
 DUSA (Ours) 	$56.6_{\pm 0.2}$	$57.9_{\pm 0.2}$	$57.0_{\pm 0.0}$	$53.3_{\pm 0.1}$	$56.7_{\pm 0.3}$	$62.4_{\pm 0.1}$	$61.6_{\pm 0.1}$	$65.9_{\pm 0.1}$	65.7 $_{\pm 0.1}$	70.1 $_{\pm 0.1}$	75.3 $_{\pm 0.1}$	$60.2_{\pm 0.3}$	$67.9_{\pm 0.1}$	69.7 $_{\pm 0.1}$	$65.8_{\pm 0.1}$	63.1
• DUSA-U (Ours)	$56.3_{\pm 0.1}$	$57.6_{\pm 0.1}$	$56.7_{\pm 0.1}$	$52.5_{\pm 0.1}$	$56.4_{\pm 0.3}$	$61.9_{\pm 0.1}$	$60.4_{\pm 0.2}$	$65.8_{\pm 0.2}$	$65.4_{\pm 0.2}$	$70.0_{\pm 0.1}$	$75.3_{\pm 0.0}$	$58.7_{\pm 0.2}$	$67.8_{\pm 0.1}$	$69.4_{\pm 0.0}$	$64.3_{\pm 0.1}$	62.6
ConvNeXt-L (LN)	56.7	56.2	58.3	35.1	20.7	47.6	43.5	58.9	59.8	48.0	76.6	55.7	34.0	42.3	63.3	50.5
 Tent 	57.4	57.8	58.9	35.7	24.3	51.3	46.3	59.8	58.4	11.0	77.1	61.2	35.1	50.0	64.4	49.9
 CoTTA 	56.7	56.2	58.3	35.1	20.7	47.6	43.5	59.0	59.9	48.0	76.6	55.7	34.0	42.3	63.3	50.5
 EATA 	57.5	58.0	59.0	38.7	27.1	51.6	47.0	60.7	58.5	49.3	77.2	61.3	40.2	50.3	64.5	53.4
• SAR	57.0	56.7	58.8	37.4	26.6	50.9	46.3	60.1	57.6	12.4	77.0	61.9	37.1	51.4	64.1	50.4
 RoTTA 	57.0	56.7	58.7	35.1	21.3	48.0	44.0	59.5	60.0	48.9	76.6	56.8	34.6	43.1	63.4	50.9
 Diffusion-TTA 	58.7	59.6	58.3	50.3	48.8	<u>57.6</u>	54.8	63.3	64.8	68.6	77.4	60.9	62.0	65.6	65.5	61.1
• DUSA (Ours)	$\textbf{64.2}_{\pm0.1}$		1.0.1										$\textbf{66.1}_{\pm 0.2}$			
• DUSA-U (Ours)	$63.8_{\pm 0.1}$	$65.2_{\pm 0.0}$	$65.2_{\pm 0.1}$	$54.0_{\pm 0.1}$	$53.3_{\pm 0.2}$	$63.3_{\pm 0.1}$	$60.6_{\pm 0.1}$	$69.9_{\pm 0.1}$	$66.4_{\pm 0.1}$	$72.5_{\pm 0.2}$	$79.6_{\pm 0.0}$	$68.1_{\pm 0.0}$	$65.9_{\pm 0.2}$	$70.3_{\pm 0.2}$	$68.7_{\pm 0.1}$	65.8

Table 2: *Continual test-time adaptation* of ImageNet pre-trained ConvNext-L on ImageNet-C. The best results are in bold and runner-ups are underlined. LN is short for Layer normalization.

Time	t															
Method	Gauss.	Shot	Impul.	Defoc.	Glass	Motion	Zoom	Snow	Frost	Fog	Brit.	Contr.	Elastic	Pixel	JPEG	Avg.
ConvNeXt-L (LN)	56.7	56.2	58.3	35.1	20.7	47.6	43.5	58.9	59.8	48.0	76.6	55.7	34.0	42.3	63.3	50.5
 Tent 	57.4	60.0	62.9	38.7	32.8	53.7	50.0	60.3	60.2	67.4	77.5	64.9	23.4	52.3	64.6	55.1
 CoTTA 	56.7	56.2	58.3	35.1	20.7	47.6	43.5	59.0	59.9	48.1	76.6	55.8	34.1	42.3	63.3	50.5
• SAR	57.0	59.6	62.6	40.9	32.5	55.1	51.1	61.1	61.2	68.3	78.0	65.4	28.4	52.1	65.2	55.9
 EATA 	57.6	61.0	63.5	42.5	35.2	55.3	52.4	62.3	62.9	68.6	78.3	66.1	46.2	56.7	66.9	58.3
 RoTTA 	57.0	58.2	60.9	34.2	24.5	47.9	45.3	60.9	62.5	51.7	74.9	49.8	39.3	42.6	62.5	51.5
 Diffusion-TTA 	58.1	63.2	63.2	54.1	56.6	61.8	62.5	65.2	65.5	68.1	75.3	58.9	37.3	54.8	60.9	60.4
 DUSA (Ours) 	$64.1_{\pm 0.1}$	$67.7_{\pm 0.0}$	$68.3_{\pm 0.1}$	$54.8_{\pm 0.3}$	$56.2_{\pm 0.2}$	$64.6_{\pm 0.0}$	$65.6_{\pm 0.1}$	$69.8_{\pm 0.0}$	$69.9_{\pm 0.2}$	$74.5_{\pm 0.1}$	79.0 $_{\pm0.1}$	$70.3_{\pm 0.0}$	$68.5_{\pm 0.1}$	$71.9_{\pm 0.1}$	70.7 $_{\pm 0.2}$	67.7

Diffusion-TTA by +2.0%, +4.5%, +5.1% on these classifiers, justifying the exploration of semantic priors underneath the diffusion score estimations and demonstrating a clear superiority of our DUSA.

Furthermore, a thrilling finding is that our DUSA is not reliant on the integration of task model prediction in objective Eq. (10) to maintain the powerful semantic priors implicitly embedded. In Table 1, we provide the adaptation results from Eq. (13), namely DUSA-U. Despite the diffusion model being trained unconditionally in DUSA-U and thus having no chance to borrow knowledge from task models, the performance is still on par with DUSA. This reinforces our conviction that diffusion models inherently possess such semantic priors, even without explicit inclusion of task models. Although DUSA-U is more lightweight (diffusion model only trained on null condition), we stick to DUSA when benchmarking against Diffusion-TTA to ensure fairness in the training budget b.

4.2 Continual Test-Time Adaptation of ImageNet Pre-trained Classifiers

We also experiment under the online continual test-time adaptation protocol, where the task model should adapt to continually changing scenarios [45]. The outcomes are reported in Table 2. Our DUSA withstands a long period of adaptation and outperforms Diffusion-TTA by a large margin of +7.3% on ConvNeXt-L. During adaptation, Diffusion-TTA witnesses a performance drop when the OOD datastream type shifts from Weather (Brit.) to Digital (Contr.), while our DUSA shows remarkable adaptation stability. This suggests that DUSA effectively learns from robust and transferable semantic priors from score-based generative modeling, allowing it to shine over prolonged adaptation.

4.3 Fully Test-Time Adaptation of ADE20K Pre-trained Segmentors

The versatility of our DUSA to dense prediction tasks is evaluated by fully test-time semantic segmentation on the ADE20K dataset with corruptions. We experiment on SegFormer-B5 and report

Table 3: *Test-time semantic segmentation* of ADE20K pre-trained SegFormer-B5 on ADE20K-C. The best results are in bold and runner-ups are underlined. LN/BN is short for Layer/Batch normalization.

	Noise			Blur				Weather				Digital				
Method	Gauss.	Shot	Impul.	Defoc.	Glass	Motion	Zoom	Snow	Frost	Fog	Brit.	Contr.	Elastic	Pixel	JPEG	Avg.
Segformer-B5 (LN+BN)	14.2	15.8	15.6	23.1	16.8	22.5	10.3	22.3	21.5	38.6	42.0	23.1	24.5	33.1	35.3	23.9
 BN Adapt 	10.8	12.0	11.7	16.6	12.8	16.6	7.9	17.0	16.8	29.6	32.4	18.2	19.2	25.5	26.3	18.2
 Tent 	11.2	13.0	12.5	17.0	13.5	16.9	7.7	17.7	17.4	29.7	32.5	18.6	20.0	25.8	26.4	18.7
 CoTTA 	14.6	16.1	15.8	22.6	16.5	22.1	9.8	20.9	20.4	38.8	42.3	21.9	24.3	33.6	35.4	23.7
• DUSA (Ours)	$23.6_{\pm 1.3}$	24.5 _{±1.0}	$23.2_{\pm 0.3}$	$\textbf{24.7}_{\pm 0.5}$	$23.2_{\pm 1.2}$	$24.7_{\pm 0.6}$	$\textbf{12.5}_{\pm 0.6}$	$27.3_{\pm 1.2}$	$\textbf{26.7}_{\pm 0.8}$	39.3 _{±0.2}	42.6 _{±0.3}	$27.1_{\pm 1.2}$	$\textbf{30.6}_{\pm 0.6}$	$35.7_{\pm 0.7}$	35.6 _{±0.7}	28.1

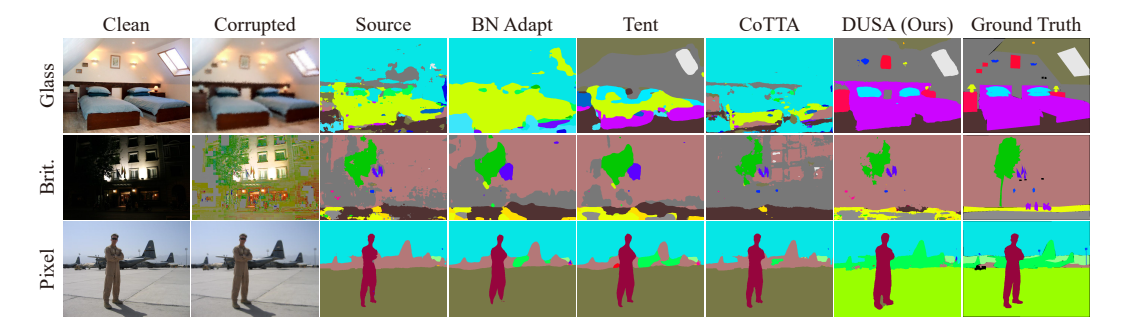
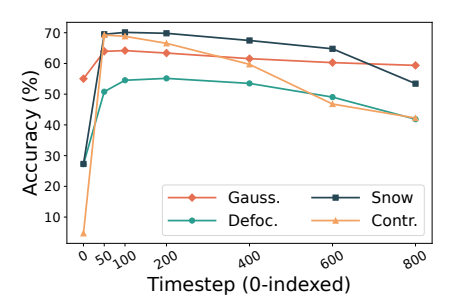


Figure 2: Visualization of segmentation results on ADE20K-C. From left to right: clean and corrupted images, results of the source model, BN Adapt, Tent, CoTTA, our DUSA, and ground-truth labels.

the results in Table 3. Notably, previous methods fail on most tasks, except for CoTTA which achieves modest improvements on a few tasks through a combination of stochastic weight restoration and data augmentation. For all tasks involved, our DUSA takes the lead by exploiting the semantic priors from the high-dimensional latent space of a pre-trained **text-to-image** diffusion model, justifying the extensiveness of our proposition to a wider range of discriminative tasks beyond classification. Segmentation results for all the methods involved are visualized in Fig. 2. Our DUSA, as shown in the illustration, showcases its ability to address errors by incorporating semantic priors from diffusion models, overcoming a limitation faced by other methods that depend solely on the task model's precision. We provide more visualizations over a wide range of scenarios in Appendix I.

4.4 Ablation Study

Selection of timestep t. As discussed in Sec. 3.2, our DUSA significantly reduces the number of timesteps to a single timestep of diffusion models. Fig. 3 illustrates the influence of timestep selection on DUSA through adapting the ConvNeXt-L classifier to corruptions from the four main categories. Consistent with our analysis in Sec. 3.3, the guidance from diffusion models is far from perfect when the chosen timestep is either too small $(t \to 0)$ or too large $(t \to T)$. We empirically find that t = 100 shows a good performance here, and generalizes well to other backbones and tasks as well. The other timesteps, e.g., t = 50, however also emerge as strong contenders and outperform Diffusion-TTA by a considerable margin. For simplicity, we adopt t = 100 in all our experiments.



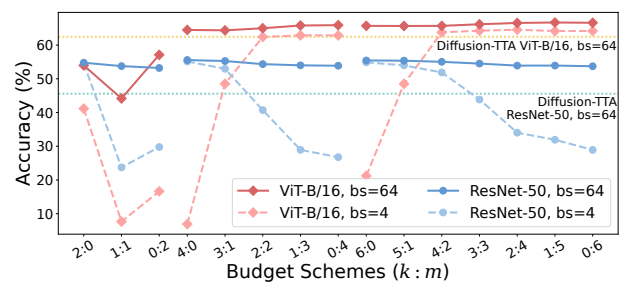


Figure 3: Accuracy of ConvNeXt-L across different selections of timestep.

Figure 4: Accuracy of ViT-B/16 on JPEG and ResNet-50 on Contrast, across different budgets for adaptation.

Effect of components in DUSA. To grasp a deeper understanding of DUSA, we provide a detailed ablation of critical designs in Table 4, where the number in parentheses means the budget b=k+m allowed for diffusion model forward (D.F.) in Eq. (10), i.e., number of classes to adapt for each sample. The results are obtained on ResNet-50 and ConvNeXt-L over the corruptions within the Noise category. We also include Pixelate corruption results on ConvNeXt-L to offer a well-rounded understanding, upon which the transferability of diffusion models to OOD data is demonstrated.

Before adaptation, the source-only models serve as the baseline. Introducing the objective in Eq. (10) when freezing the diffusion model brings about a performance gain of +3.6% on ResNet-50 for Noise, but causes a degradation of -13% on ConvNeXt-L. This is largely due to the instability from discarding classes, as pointed out in Sec. 3.3. Applying LogitNorm instantly mitigates the issue and brings about a consistent gain of +21.6% and +3.8% against baselines. The im-

Table 4: Ablation on critical components in DUSA. Components in colored rows are not carried over to subsequent rows.

					ResNet-50	ConvN	eXt-L
Variants	k	m	D.F.	D.B.	Noise	Noise	Pixel
Source-only	0	0	0	0	22.4	57.1	42.3
+ score priors inspired loss (4)	4	0	4	0	26.0	44.1	9.2
+ LogitNorm (4)	4	0	4	0	44.0	60.9	9.6
+ adapt diffusion (4)	4	0	4	4	41.2	57.8	49.3
+ LogitNorm (4)	4	0	4	4	46.4	65.0	70.4
+ LogitNorm (6)	6	0	6	6	46.5	65.1	70.7
+ uniform select (6)	4	2	6	6	46.2	65.1	70.7
+ multinomial select (6) (DUSA)	4	2	6	6	46.3	65.1	70.8
+ null conditioning (6) (DUSA-U)	4	2	7	1	46.1	64.7	70.5

provement is made without training diffusion models and therefore can be viewed as exploiting the generative semantic priors formed in diffusion pre-training. However, the outcomes are still below the baseline for Pixelate. We conjecture that such corruption might be OOD even for a diffusion model with strong robustness. The further adaptation of diffusion models removes this concern, pushing all results to a competitive level. We attribute this finding to the fast convergence of generative modeling [1] on unseen data, which is favorable to the online nature of test-time adaptation. Again, the inclusion of LogitNorm yields a significantly boosted accuracy at 46.4%, 65.0% and 70.4%.

To provide a basis for the further ablation of budget schemes, the budget is raised from 4 to 6 with a slight increase in performance. A mild drop in accuracy is witnessed when handing the class bias problem in Sec. 3.3 with a budget m=2 used with uniform sampling, which is then improved by our multinomial selection in the penultimate line. We underline that such a design is indispensable for a small batch size, which is also practical [59]. For better consistency, k=4, m=2 are universally adopted for DUSA in classification, the ratio between them to be delved into below. Interestingly, with access to a diffusion model capable of unconditional generation, DUSA-U could achieve performance comparable to DUSA using Eq. (13), while significantly reducing the computational cost associated with diffusion model backward (D.B.). We believe this observation can back our claim of the existence of structured semantic priors inherently embedded in diffusion models.

Specifying a budget scheme. As a justification for our design of the selection strategies in CSM, we take a thorough investigation into the effects of different budget schemes over varied classifiers (ResNet-50 & ViT-B/16) and batch size (4 & 64) in Fig. 4. At a smaller batch size (bs) of 4 (dashed lines), the budget scheme k:m plays a vital role in performance. Concretely, a large k is favorable to weaker task models (ResNets) for eager adaptation, while a proper m is a must to prevent more powerful ones (ViTs) from overfitting to a subset of classes. When the batch size is increased to the standard 64 (solid lines), our DUSA becomes insensitive to budget schemes, and a consistent gain is observed for both classifiers. DUSA with b=4 even exceeds Diffusion-TTA with b=6, underscoring the advanced efficiency made possible by our proposition and practical designs. For a budget scheme, we find m=2 competitive across varied b, and stick to k=4, m=2 for DUSA.

5 Related Work

Test-time adaptation. Test-time adaptation [44] focuses on improving source data pre-trained model performance on out-of-distribution target data without label access during inference time. Early works lay more emphasis on adapting the activation statistics of batch normalization (BN) [62, 63, 66, 67]. Test-time training [68, 69, 70, 71] methods manage to adapt through devising a test-time self-supervised objective which is also injected into the pre-training stage, resulting in complicated pipelines and increased computational cost. To lessen dependence on source data and extra loss

injection, fully test-time adaptation [44] is advocated to achieve adaptation with only unlabeled target data. Concretely, previous works are majorly based on entropy minimization objectives: Tent [44] directly minimizes entropy on batched data predictions, MEMO [72] proposes marginal entropy minimization via data augmentation, EATA [60] pursues a sample efficient entropy minimization and anti-forgetting regularization, while SAR [59] advocates sharpness-aware and reliable entropy minimization. Other works delve into extensive distributional shifts in TTA [73], e.g., continual adaptation without forgetting [45, 60], correlative data streams [61] and label shifts [59, 74]. Our DUSA is much different as it is not reliant on error-prone entropy-based objectives and rather extracts knowledge from semantic priors of generative models for better adaptation of the task model.

Generative models for discriminative tasks. The long-standing discussion on the connections between generative and discriminative models [1, 75, 76] has inspired a handful of attempts to integrate the two seemingly disparate paradigms [2, 3, 4, 19, 77, 78, 79, 80]. Specifically, a collection of works showcase the impressive power of generative pre-training followed by supervised finetuning [15, 24, 27, 81, 82, 83, 84]. Besides, a few works utilize generative models as zero-shot recognizers [25, 29, 85]. Integrating generative modeling into the task of test-time adaptation is gaining traction. Prior works manage to boost task model performance with a variety of generative techniques, including GANs [86], MAEs [87], energy-based [88] and flow-based [89]. The recent prevalence of diffusion models with extraordinary generation capability stimulates a range of works on adapting them for discriminative tasks. As for TTA, two distinct research directions arise. Appreciating the generative power [90, 91] of diffusion models, a series of works propose to adapt samples in the input space [92, 93, 94]. Another largely under-explored direction is to repurpose the generative objective of diffusion models as a proxy of discriminative ability enhancement, with Diffusion-TTA [32] pioneering in incorporating task predictions into the class condition of denoising objective in an inversion [7, 25, 29, 95] style. Our DUSA belongs to the latter direction but is fundamentally different from [32], in that we delve deeper into the semantic priors of diffusion models from the perspective of score functions and achieve better adaptability and versatility.

Timestep selection in diffusion models. The importance of timestep selection in diffusion models has been widely recognized in the literature. In image editing tasks, diffusion models are observed to exhibit a natural coarse-to-fine pattern during the reverse process [91, 96, 97, 98, 99, 100]. Consequently, the trade-off between realism and fidelity in editing largely stems from the chosen intervals of timesteps. In discriminative tasks, timestep selection is also crucial to the quality of extracted features. An early study [83] elucidated the features within diffusion models, revealing that the most informative ones are derived from smaller timesteps. Subsequent works have reinforced this finding by utilizing a single small timestep across various tasks, including semantic segmentation, referring image segmentation, depth estimation [24], object detection [26], semantic correspondence [101], and one-shot image segmentation [102]. While our DUSA aligns with the existing literature on using a single timestep, it differs by extracting semantic priors rather than focusing on feature extraction.

6 Conclusion

In this paper, we introduce DUSA, a competitive test-time adaptation method built on the structured semantic priors underlying diffusion models, which serve as score estimators. A proposition is offered to unveil the semantic structure in these score-based models, upon which a test-time objective is derived to fully exploit the implicit semantic priors. Our approach is also shown to generalize well to modern diffusion models and dense prediction tasks. Additionally, we enhance the adaptation efficiency through a few practical designs. The effectiveness of our DUSA is demonstrated across three challenging benchmarks, where it consistently outperforms competing methods. We hope our method will pave the way for better utilization of generative modeling for discriminative tasks.

Acknowledgments and Disclosure of Funding

This paper was supported by the National Natural Science Foundation of China (No. 62376026), Beijing Nova Program (No. 20230484296) and KuaiShou.

References

- [1] Andrew Ng and Michael Jordan. On discriminative vs. generative classifiers: A comparison of logistic regression and naive bayes. In *NeurIPS*, pages 841–848, 2001.
- [2] Rajat Raina, Yirong Shen, Andrew Y. Ng, and Andrew McCallum. Classification with hybrid generative/discriminative models. In *NeurIPS*, pages 545–552, 2003.
- [3] Victor Garcia Satorras, Zeynep Akata, and Max Welling. Combining generative and discriminative models for hybrid inference. In *NeurIPS*, pages 13802–13812, 2019.
- [4] Will Grathwohl, Kuan-Chieh Wang, Joern-Henrik Jacobsen, David Duvenaud, Mohammad Norouzi, and Kevin Swersky. Your classifier is secretly an energy based model and you should treat it like one. In *ICLR*, 2020.
- [5] Kaiming He, Xiangyu Zhang, Shaoqing Ren, and Jian Sun. Deep residual learning for image recognition. In *CVPR*, pages 770–778, 2016.
- [6] Zhuang Liu, Hanzi Mao, Chao-Yuan Wu, Christoph Feichtenhofer, Trevor Darrell, and Saining Xie. A convnet for the 2020s. In CVPR, pages 11976–11986, 2022.
- [7] Rinon Gal, Yuval Alaluf, Yuval Atzmon, Or Patashnik, Amit Haim Bermano, Gal Chechik, and Daniel Cohen-or. An image is worth one word: Personalizing text-to-image generation using textual inversion. In *ICLR*, 2023.
- [8] Le Yang, Haojun Jiang, Ruojin Cai, Yulin Wang, Shiji Song, Gao Huang, and Qi Tian. Condensenet v2: Sparse feature reactivation for deep networks. In *Proceedings of the IEEE/CVF Conference on Computer Vision and Pattern Recognition*, pages 3569–3578, 2021.
- [9] Le Yang, Yizeng Han, Xi Chen, Shiji Song, Jifeng Dai, and Gao Huang. Resolution adaptive networks for efficient inference. In *Proceedings of the IEEE/CVF conference on computer vision and pattern* recognition, pages 2369–2378, 2020.
- [10] Ziwei Zheng, Le Yang, Yulin Wang, Miao Zhang, Lijun He, Gao Huang, and Fan Li. Dynamic spatial focus for efficient compressed video action recognition. *IEEE Transactions on Circuits and Systems for Video Technology*, 2024.
- [11] Le Yang, Ziwei Zheng, Jian Wang, Shiji Song, Gao Huang, and Fan Li. Adadet: An adaptive object detection system based on early-exit neural networks. *IEEE Transactions on Cognitive and Developmental Systems*, 16(1):332–345, 2023.
- [12] Sara Beery, Grant Van Horn, and Pietro Perona. Recognition in terra incognita. In *ECCV*, pages 456–473,
- [13] Robert Geirhos, Jörn-Henrik Jacobsen, Claudio Michaelis, Richard Zemel, Wieland Brendel, Matthias Bethge, and Felix A Wichmann. Shortcut learning in deep neural networks. *Nat. Mach. Intell.*, 2(11):665–673, 2020.
- [14] Xi Chen, Yan Duan, Rein Houthooft, John Schulman, Ilya Sutskever, and Pieter Abbeel. Infogan: Interpretable representation learning by information maximizing generative adversarial nets. In *NeurIPS*, pages 2172–2180, 2016.
- [15] Kaiming He, Xinlei Chen, Saining Xie, Yanghao Li, Piotr Dollár, and Ross Girshick. Masked autoencoders are scalable vision learners. In CVPR, pages 16000–16009, 2022.
- [16] Sarthak Mittal, Korbinian Abstreiter, Stefan Bauer, Bernhard Schölkopf, and Arash Mehrjou. Diffusion based representation learning. In *ICML*, pages 24963–24982, 2023.
- [17] Xuwang Yin, Soheil Kolouri, and Gustavo K Rohde. Gat: Generative adversarial training for adversarial example detection and robust classification. In *ICLR*, 2020.
- [18] Xuwang Yin. Generative robust classification. arXiv preprint arXiv:2212.07283, 2022.
- [19] Tianhong Li, Huiwen Chang, Shlok Mishra, Han Zhang, Dina Katabi, and Dilip Krishnan. Mage: Masked generative encoder to unify representation learning and image synthesis. In CVPR, pages 2142–2152, 2023.
- [20] Robin Rombach, Andreas Blattmann, Dominik Lorenz, Patrick Esser, and Björn Ommer. High-resolution image synthesis with latent diffusion models. In CVPR, pages 10684–10695, 2022.
- [21] Chitwan Saharia, William Chan, Saurabh Saxena, Lala Li, Jay Whang, Emily Denton, Seyed Kam-yar Seyed Ghasemipour, Raphael Gontijo-Lopes, Burcu Karagol Ayan, Tim Salimans, Jonathan Ho, David J. Fleet, and Mohammad Norouzi. Photorealistic text-to-image diffusion models with deep language understanding. In *NeurIPS*, pages 36479–36494, 2022.
- [22] William Peebles and Saining Xie. Scalable diffusion models with transformers. In *ICCV*, pages 4195–4205, 2023.

- [23] Soumik Mukhopadhyay, Matthew Gwilliam, Yosuke Yamaguchi, Vatsal Agarwal, Namitha Padmanabhan, Archana Swaminathan, Tianyi Zhou, and Abhinav Shrivastava. Do text-free diffusion models learn discriminative visual representations? *arXiv* preprint arXiv:2311.17921, 2023.
- [24] Wenliang Zhao, Yongming Rao, Zuyan Liu, Benlin Liu, Jie Zhou, and Jiwen Lu. Unleashing text-to-image diffusion models for visual perception. In *ICCV*, pages 5729–5739, 2023.
- [25] Alexander C. Li, Mihir Prabhudesai, Shivam Duggal, Ellis Brown, and Deepak Pathak. Your diffusion model is secretly a zero-shot classifier. In *ICCV*, pages 2206–2217, 2023.
- [26] Manlin Zhang, Jie Wu, Yuxi Ren, Ming Li, Jie Qin, Xuefeng Xiao, Wei Liu, Rui Wang, Min Zheng, and Andy J Ma. Diffusionengine: Diffusion model is scalable data engine for object detection. arXiv preprint arXiv:2309.03893, 2023.
- [27] Jiarui Xu, Sifei Liu, Arash Vahdat, Wonmin Byeon, Xiaolong Wang, and Shalini De Mello. Open-vocabulary panoptic segmentation with text-to-image diffusion models. In CVPR, pages 2955–2966, 2023.
- [28] Junyi Zhang, Charles Herrmann, Junhwa Hur, Luisa Polania Cabrera, Varun Jampani, Deqing Sun, and Ming-Hsuan Yang. A tale of two features: Stable diffusion complements dino for zero-shot semantic correspondence. *NeurIPS*, 36, 2024.
- [29] Kevin Clark and Priyank Jaini. Text-to-image diffusion models are zero shot classifiers. In *NeurIPS*, pages 58921–58937, 2023.
- [30] Priyank Jaini, Kevin Clark, and Robert Geirhos. Intriguing properties of generative classifiers. In *ICLR*, 2024.
- [31] Dan Hendrycks and Thomas Dietterich. Benchmarking neural network robustness to common corruptions and perturbations. In *ICLR*, 2019.
- [32] Mihir Prabhudesai, Tsung-Wei Ke, Alexander Cong Li, Deepak Pathak, and Katerina Fragkiadaki. Test-time adaptation of discriminative models via diffusion generative feedback. In *NeurIPS*, 2023.
- [33] René Haas, Inbar Huberman-Spiegelglas, Rotem Mulayoff, and Tomer Michaeli. Discovering interpretable directions in the semantic latent space of diffusion models. *arXiv preprint arXiv:2303.11073*, 2023.
- [34] Mingi Kwon, Jaeseok Jeong, and Youngjung Uh. Diffusion models already have a semantic latent space. In ICLR, 2023.
- [35] Yusuf Dalva and Pinar Yanardag. Noiseclr: A contrastive learning approach for unsupervised discovery of interpretable directions in diffusion models. arXiv preprint arXiv:2312.05390, 2023.
- [36] Jiafeng Mao, Xueting Wang, and Kiyoharu Aizawa. Guided image synthesis via initial image editing in diffusion model. In *ACM MM*, pages 5321–5329, 2023.
- [37] Yong-Hyun Park, Mingi Kwon, Jaewoong Choi, Junghyo Jo, and Youngjung Uh. Understanding the latent space of diffusion models through the lens of riemannian geometry. In *NeurIPS*, 2023.
- [38] Jonathan Ho, Ajay Jain, and Pieter Abbeel. Denoising diffusion probabilistic models. In *NeurIPS*, pages 6840–6851, 2020.
- [39] Pascal Vincent. A connection between score matching and denoising autoencoders. *Neural Comput.*, 23(7):1661–1674, 2011.
- [40] Yang Song and Stefano Ermon. Generative modeling by estimating gradients of the data distribution. In *NeurIPS*, pages 11895–11907, 2019.
- [41] Yang Song and Stefano Ermon. Improved techniques for training score-based generative models. In *NeurIPS*, pages 12438–12448, 2020.
- [42] Yang Song, Jascha Sohl-Dickstein, Diederik P. Kingma, Abhishek Kumar, Stefano Ermon, and Ben Poole. Score-based generative modeling through stochastic differential equations. In *ICLR*, 2021.
- [43] Calvin Luo. Understanding diffusion models: A unified perspective. arXiv preprint arXiv:2208.11970, 2022.
- [44] Dequan Wang, Evan Shelhamer, Shaoteng Liu, Bruno Olshausen, and Trevor Darrell. Tent: Fully test-time adaptation by entropy minimization. In *ICLR*, 2021.
- [45] Qin Wang, Olga Fink, Luc Van Gool, and Dengxin Dai. Continual test-time domain adaptation. In CVPR, pages 7201–7211, 2022.
- [46] Jascha Sohl-Dickstein, Eric Weiss, Niru Maheswaranathan, and Surya Ganguli. Deep unsupervised learning using nonequilibrium thermodynamics. In *ICML*, pages 2256–2265, 2015.
- [47] Alexander Quinn Nichol, Prafulla Dhariwal, Aditya Ramesh, Pranav Shyam, Pamela Mishkin, Bob Mcgrew, Ilya Sutskever, and Mark Chen. GLIDE: Towards photorealistic image generation and editing with text-guided diffusion models. In *ICML*, pages 16784–16804, 2022.

- [48] Lvmin Zhang, Anyi Rao, and Maneesh Agrawala. Adding conditional control to text-to-image diffusion models. In ICCV, pages 3836–3847, 2023.
- [49] Bradley Efron. Tweedie's formula and selection bias. JASA, 106(496):1602–1614, 2011.
- [50] Tim Salimans and Jonathan Ho. Progressive distillation for fast sampling of diffusion models. In *ICLR*, 2022.
- [51] Yang Song and Diederik P Kingma. How to train your energy-based models. *arXiv preprint* arXiv:2101.03288, 2021.
- [52] Valentin De Bortoli, Michael Hutchinson, Peter Wirnsberger, and Arnaud Doucet. Target score matching. arXiv preprint arXiv:2402.08667, 2024.
- [53] Mihir Prabhudesai, Tsung-Wei Ke, Alexander Cong Li, Deepak Pathak, and Katerina Fragkiadaki. Test-time adaptation with diffusion models. In *ICML Workshop*, 2023.
- [54] Hongxin Wei, Renchunzi Xie, Hao Cheng, Lei Feng, Bo An, and Yixuan Li. Mitigating neural network overconfidence with logit normalization. In *ICML*, pages 23631–23644, 2022.
- [55] Mingjia Li, Binhui Xie, Shuang Li, Chi Harold Liu, and Xinjing Cheng. Vblc: Visibility boosting and logit-constraint learning for domain adaptive semantic segmentation under adverse conditions. In AAAI, pages 8605–8613, 2023.
- [56] Bolei Zhou, Hang Zhao, Xavier Puig, Sanja Fidler, Adela Barriuso, and Antonio Torralba. Scene parsing through ade20k dataset. In CVPR, pages 633–641, 2017.
- [57] Alexey Dosovitskiy, Lucas Beyer, Alexander Kolesnikov, Dirk Weissenborn, Xiaohua Zhai, Thomas Unterthiner, Mostafa Dehghani, Matthias Minderer, Georg Heigold, Sylvain Gelly, Jakob Uszkoreit, and Neil Houlsby. An image is worth 16x16 words: Transformers for image recognition at scale. In *ICLR*, 2021.
- [58] Enze Xie, Wenhai Wang, Zhiding Yu, Anima Anandkumar, Jose M. Alvarez, and Ping Luo. Segformer: Simple and efficient design for semantic segmentation with transformers. In *NeurIPS*, pages 12077–12090, 2021.
- [59] Shuaicheng Niu, Jiaxiang Wu, Yifan Zhang, Zhiquan Wen, Yaofo Chen, Peilin Zhao, and Mingkui Tan. Towards stable test-time adaptation in dynamic wild world. In *ICLR*, 2023.
- [60] Shuaicheng Niu, Jiaxiang Wu, Yifan Zhang, Yaofo Chen, Shijian Zheng, Peilin Zhao, and Mingkui Tan. Efficient test-time model adaptation without forgetting. In *ICML*, pages 16888–16905, 2022.
- [61] Longhui Yuan, Binhui Xie, and Shuang Li. Robust test-time adaptation in dynamic scenarios. In CVPR, pages 15922–15932, 2023.
- [62] Zachary Nado, Shreyas Padhy, D Sculley, Alexander D'Amour, Balaji Lakshminarayanan, and Jasper Snoek. Evaluating prediction-time batch normalization for robustness under covariate shift. arXiv preprint arXiv:2006.10963, 2020.
- [63] Steffen Schneider, Evgenia Rusak, Luisa Eck, Oliver Bringmann, Wieland Brendel, and Matthias Bethge. Improving robustness against common corruptions by covariate shift adaptation. In *NeurIPS*, pages 11539–11551, 2020.
- [64] Diederik Kingma and Jimmy Ba. Adam: A method for stochastic optimization. In ICLR, 2015.
- [65] Jia Deng, Wei Dong, Richard Socher, Li-Jia Li, Kai Li, and Li Fei-Fei. Imagenet: A large-scale hierarchical image database. In CVPR, pages 248–255, 2009.
- [66] Yanghao Li, Naiyan Wang, Jianping Shi, Jiaying Liu, and Xiaodi Hou. Revisiting batch normalization for practical domain adaptation. In *ICLR Workshop*, 2017.
- [67] Ansh Khurana, Sujoy Paul, Piyush Rai, Soma Biswas, and Gaurav Aggarwal. Sita: Single image test-time adaptation. *arXiv preprint arXiv:2112.02355*, 2021.
- [68] Yu Sun, Xiaolong Wang, Zhuang Liu, John Miller, Alexei Efros, and Moritz Hardt. Test-time training with self-supervision for generalization under distribution shifts. In *ICML*, pages 9229–9248, 2020.
- [69] Yuejiang Liu, Parth Kothari, Bastien Germain van Delft, Baptiste Bellot-Gurlet, Taylor Mordan, and Alexandre Alahi. TTT++: When does self-supervised test-time training fail or thrive? In NeurIPS, 2021.
- [70] Yossi Gandelsman, Yu Sun, Xinlei Chen, and Alexei A Efros. Test-time training with masked autoencoders. In Alice H. Oh, Alekh Agarwal, Danielle Belgrave, and Kyunghyun Cho, editors, *NeurIPS*, 2022.
- [71] Alexander Bartler, Andre Bühler, Felix Wiewel, Mario Döbler, and Bin Yang. Mt3: Meta test-time training for self-supervised test-time adaption. In *AISTATS*, pages 3080–3090, 2022.
- [72] Marvin Mengxin Zhang, Sergey Levine, and Chelsea Finn. MEMO: Test time robustness via adaptation and augmentation. In *NeurIPS*, pages 38629–38642, 2022.

- [73] Hao Zhao, Yuejiang Liu, Alexandre Alahi, and Tao Lin. On pitfalls of test-time adaptation. In *ICML*, pages 42058–42080, 2023.
- [74] Malik Boudiaf, Romain Mueller, Ismail Ben Ayed, and Luca Bertinetto. Parameter-free online test-time adaptation. In CVPR, pages 8344–8353, 2022.
- [75] Jing-Hao Xue and D Michael Titterington. Comment on "on discriminative vs. generative classifiers: A comparison of logistic regression and naive bayes". *Neural Process. Lett.*, 28:169–187, 2008.
- [76] Chenyu Zheng, Guoqiang Wu, Fan Bao, Yue Cao, Chongxuan Li, and Jun Zhu. Revisiting discriminative vs. generative classifiers: Theory and implications. In *ICML*, pages 42420–42477, 2023.
- [77] Anh Nguyen, Jeff Clune, Yoshua Bengio, Alexey Dosovitskiy, and Jason Yosinski. Plug & play generative networks: Conditional iterative generation of images in latent space. In *CVPR*, pages 4467–4477, 2017.
- [78] Xiulong Yang and Shihao Ji. Jem++: improved techniques for training jem. In *ICCV*, pages 6494–6503, 2021.
- [79] Xiulong Yang, Sheng-Min Shih, Yinlin Fu, Xiaoting Zhao, and Shihao Ji. Your vit is secretly a hybrid discriminative-generative diffusion model. *arXiv preprint arXiv:2208.07791*, 2022.
- [80] Tianhong Li, Dina Katabi, and Kaiming He. Return of unconditional generation: A self-supervised representation generation method. *arXiv preprint arXiv:2312.03701*, 2023.
- [81] Jeff Donahue, Philipp Krähenbühl, and Trevor Darrell. Adversarial feature learning. *arXiv preprint arXiv:1605.09782*, 2016.
- [82] Deepak Pathak, Philipp Krahenbuhl, Jeff Donahue, Trevor Darrell, and Alexei A Efros. Context encoders: Feature learning by inpainting. In *CVPR*, pages 2536–2544, 2016.
- [83] Dmitry Baranchuk, Andrey Voynov, Ivan Rubachev, Valentin Khrulkov, and Artem Babenko. Labelefficient semantic segmentation with diffusion models. In ICLR, 2022.
- [84] Mannat Singh, Quentin Duval, Kalyan Vasudev Alwala, Haoqi Fan, Vaibhav Aggarwal, Aaron Adcock, Armand Joulin, Piotr Dollár, Christoph Feichtenhofer, Ross Girshick, et al. The effectiveness of mae pre-pretraining for billion-scale pretraining. In *ICCV*, pages 5484–5494, 2023.
- [85] Ryan Burgert, Kanchana Ranasinghe, Xiang Li, and Michael S Ryoo. Peekaboo: Text to image diffusion models are zero-shot segmentors. arXiv preprint arXiv:2211.13224, 2022.
- [86] Rui Li, Qianfen Jiao, Wenming Cao, Hau-San Wong, and Si Wu. Model adaptation: Unsupervised domain adaptation without source data. In CVPR, pages 9641–9650, 2020.
- [87] Jiaming Liu, Ran Xu, Senqiao Yang, Renrui Zhang, Qizhe Zhang, Zehui Chen, Yandong Guo, and Shanghang Zhang. Adaptive distribution masked autoencoders for continual test-time adaptation. *arXiv* preprint arXiv:2312.12480, 2023.
- [88] Yige Yuan, Bingbing Xu, Liang Hou, Fei Sun, Huawei Shen, and Xueqi Cheng. Tea: Test-time energy adaptation. *arXiv preprint arXiv:2311.14402*, 2023.
- [89] David Osowiechi, Gustavo A Vargas Hakim, Mehrdad Noori, Milad Cheraghalikhani, Ismail Ben Ayed, and Christian Desrosiers. Tttflow: Unsupervised test-time training with normalizing flow. In WACV, pages 2126–2134, 2023.
- [90] Jonathan Ho and Tim Salimans. Classifier-free diffusion guidance. arXiv preprint arXiv:2207.12598, 2022.
- [91] Chenlin Meng, Yutong He, Yang Song, Jiaming Song, Jiajun Wu, Jun-Yan Zhu, and Stefano Ermon. SDEdit: Guided image synthesis and editing with stochastic differential equations. In *ICLR*, 2022.
- [92] Weili Nie, Brandon Guo, Yujia Huang, Chaowei Xiao, Arash Vahdat, and Anima Anandkumar. Diffusion models for adversarial purification. In *ICML*, pages 16805–16827, 2022.
- [93] Jin Gao, Jialing Zhang, Xihui Liu, Trevor Darrell, Evan Shelhamer, and Dequan Wang. Back to the source: Diffusion-driven adaptation to test-time corruption. In *CVPR*, pages 11786–11796, 2023.
- [94] Kaiyu Song and Hanjiang Lai. Target to source: Guidance-based diffusion model for test-time adaptation. *arXiv preprint arXiv:2312.05274*, 2023.
- [95] Ron Mokady, Amir Hertz, Kfir Aberman, Yael Pritch, and Daniel Cohen-Or. Null-text inversion for editing real images using guided diffusion models. In CVPR, pages 6038–6047, 2023.
- [96] Jooyoung Choi, Sungwon Kim, Yonghyun Jeong, Youngjune Gwon, and Sungroh Yoon. Ilvr: Conditioning method for denoising diffusion probabilistic models. arXiv preprint arXiv:2108.02938, 2021.
- [97] Giannis Daras and Alexandros G Dimakis. Multiresolution textual inversion. *arXiv preprint* arXiv:2211.17115, 2022.
- [98] Yogesh Balaji, Seungjun Nah, Xun Huang, Arash Vahdat, Jiaming Song, Qinsheng Zhang, Karsten Kreis, Miika Aittala, Timo Aila, Samuli Laine, et al. ediff-i: Text-to-image diffusion models with an ensemble of expert denoisers. *arXiv preprint arXiv:2211.01324*, 2022.

- [99] Hila Chefer, Yuval Alaluf, Yael Vinker, Lior Wolf, and Daniel Cohen-Or. Attend-and-excite: Attention-based semantic guidance for text-to-image diffusion models. *TOG*, 42(4):1–10, 2023.
- [100] Andrey Voynov, Kfir Aberman, and Daniel Cohen-Or. Sketch-guided text-to-image diffusion models. In *SIGGRAPH*, pages 1–11, 2023.
- [101] Eric Hedlin, Gopal Sharma, Shweta Mahajan, Hossam Isack, Abhishek Kar, Andrea Tagliasacchi, and Kwang Moo Yi. Unsupervised semantic correspondence using stable diffusion. Advances in Neural Information Processing Systems, 36, 2024.
- [102] Aliasghar Khani, Saeid Asgari, Aditya Sanghi, Ali Mahdavi Amiri, and Ghassan Hamarneh. SLime: Segment like me. In ICLR, 2024.
- [103] MMPreTrain Contributors. Openmmlab's pre-training toolbox and benchmark. https://github.com/open-mmlab/mmpretrain, 2023.
- [104] MMSegmentation Contributors. MMSegmentation: Openmmlab semantic segmentation toolbox and benchmark. https://github.com/open-mmlab/mmsegmentation, 2020.
- [105] Claudio Michaelis, Benjamin Mitzkus, Robert Geirhos, Evgenia Rusak, Oliver Bringmann, Alexander S. Ecker, Matthias Bethge, and Wieland Brendel. Benchmarking robustness in object detection: Autonomous driving when winter is coming. arXiv preprint arXiv:1907.07484, 2019.
- [106] Ross Wightman. Pytorch image models. https://github.com/rwightman/pytorch-image-models, 2019.

A Broader Impacts and Limitations

Broader Impacts. In this work, an approach to incorporate generative diffusion models into the discriminative task of test-time adaptation is introduced. The leverage of knowledge from generative modeling teaches a whole picture of the scenario to the task model, enabling better robustness and adaptability and is thus favorable to some relevant scenarios like medical analysis and quality control of manufacturing in varying environments. However, the adoption of generative models might come with a risk of learning from a biased source of knowledge, leading to improper decisions from the adapted task model. A possible remedy for this is to foster the research into more unbiased or balanced training of generative models.

Limitations. Our work presents an effective way of borrowing semantic priors from score-based diffusion models to benefit the discriminative task model that demands adaptation at test time without labels. We acknowledge that, as with any research endeavor, limitations exist in our work. Firstly, our competitive method involves a diffusion model pre-trained at least on the same set of source data as the task model, which may not be easily accessible for certain scenarios. However, we believe such a dilemma can be mitigated with advances in generative diffusion models, which have demonstrated remarkable progress in both generality and robustness. Our approach achieves significant adaptation efficiency gains against prior diffusion-based TTA methods, but there is still a gap in the time compared to methods that only update the task model. Therefore, it may not meet extreme efficiency demands in scenarios like autonomous driving. Our method, however, yields superior performance and is thus appealing to another set of tasks where trading a slight loss in efficiency for boosted accuracy is tolerable, e.g., non-emergent medical diagnosis. With this said, we highlight that our theoretical findings are not confined to diffusion models but extensive to all score-based models, therefore substituting a more lightweight technique in score estimation for the computationally expensive diffusion models can be a promising avenue. We leave it for future work.

B Licenses for Existing Assets

All models and datasets used in our experiments are publicly available, and their licenses are listed below. (D) means data, (M) means model, (C) means code.

- (D) ImageNet-C [31]: CC-BY 4.0
- (D) ADE20K 2016 [56]: BSD 3-clause license
- (M) ResNet-50 [5]: Apache-2.0 license
- (M) ViT-Base/16 [57]: Apache-2.0 license
- (M) ConvNeXt-L [6]: MIT license
- (M) DiT-XL/2 [22]: CC-BY-NC 4.0
- (M) Stable Diffusion v1.5 [20]: The CreativeML OpenRAIL M license
- (M) ControlNet [48]: The CreativeML OpenRAIL M license
- (C) MMPreTrain [103]: Apache-2.0 license
- (C) MMSegmentation [104]: Apache-2.0 license
- (C) Diffusion-TTA [32]: MIT license

C Proofs

Proposition 1. Let $p(\mathbf{x})$ and $\{p(\mathbf{x} \mid y) : y \in \mathcal{Y}\}$ be continuously differentiable probability densities, their score functions $\nabla_{\mathbf{x}} \log p(\mathbf{x})$ and $\{\nabla_{\mathbf{x}} \log p(\mathbf{x} \mid y) : y \in \mathcal{Y}\}$, the following equation holds:

$$\nabla_{\mathbf{x}} \log p(\mathbf{x}) = \sum_{y} p(y \mid \mathbf{x}) \nabla_{\mathbf{x}} \log p(\mathbf{x} \mid y). \tag{15}$$

Proof. The proof starts from the law of total probability. With the assumption of continuously differentiable, we can take derivatives of the probability densities on input data. Note that we always

assume the existence of x, implying that p(x) is non-zero. The complete proof is then as follows:

$$p(\mathbf{x}) = \sum_{y} p(y)p(\mathbf{x} \mid y) \qquad \text{(law of total probability)}$$

$$\nabla_{\mathbf{x}} p(\mathbf{x}) = \sum_{y} p(y)\nabla_{\mathbf{x}} p(\mathbf{x} \mid y) \qquad \text{(differentiate both sides on } \mathbf{x})$$

$$p(\mathbf{x})\nabla_{\mathbf{x}}\log p(\mathbf{x}) = \sum_{y} p(y)p(\mathbf{x} \mid y)\nabla_{\mathbf{x}}\log p(\mathbf{x} \mid y) \qquad \text{(log-derivative trick)}$$

$$p(\mathbf{x})\nabla_{\mathbf{x}}\log p(\mathbf{x}) = \sum_{y} p(\mathbf{x})p(y \mid \mathbf{x})\nabla_{\mathbf{x}}\log p(\mathbf{x} \mid y) \qquad \text{(Bayes theorem)}$$

$$\nabla_{\mathbf{x}}\log p(\mathbf{x}) = \sum_{y} p(y \mid \mathbf{x})\nabla_{\mathbf{x}}\log p(\mathbf{x} \mid y) \qquad \text{(eliminate } p(\mathbf{x}))$$

Corollary 1. Let $\epsilon \sim \mathcal{N}(\mathbf{0}, \mathbf{I})$ be a sampled noise in a forward process parameterized by $\{\bar{\alpha}_t\}_{t=1}^T$ to get noisy data \mathbf{x}_t , the connection between score function $\nabla_{\mathbf{x}_t} \log p(\mathbf{x}_t)$ and noise ϵ can be given by:

$$\nabla_{\mathbf{x}_t} \log p(\mathbf{x}_t) = -\frac{\epsilon}{\sqrt{1 - \bar{\alpha}_t}}.$$
(17)

Proof. According to the definition in Eq. (2), we have

$$q(\mathbf{x}_t \mid \mathbf{x}_0) = \mathcal{N}(\mathbf{x}_t; \sqrt{\bar{\alpha}_t} \mathbf{x}_0, (1 - \bar{\alpha}_t) \mathbf{I}). \tag{18}$$

Tweedie's Formula in Lemma 1 states that, for observed gaussian variable $\mathbf{z} \mid \boldsymbol{\mu}_{\mathbf{z}} \sim \mathcal{N}(\mathbf{z}; \boldsymbol{\mu}_{\mathbf{z}}, \boldsymbol{\Sigma}_{\mathbf{z}})$, we have the estimation

$$\mathbb{E}[\boldsymbol{\mu}_{\mathbf{z}} \mid \mathbf{z}] = \mathbf{z} + \boldsymbol{\Sigma}_{\mathbf{z}} \nabla_{\mathbf{z}} \log p(\mathbf{z}). \tag{19}$$

Applying Tweedie's Formula, we now have

$$\mathbb{E}[\boldsymbol{\mu}_{\mathbf{x}_t} \mid \mathbf{x}_t] = \mathbf{x}_t + \boldsymbol{\Sigma}_{\mathbf{x}_t} \nabla_{\mathbf{x}_t} \log p(\mathbf{x}_t)$$

$$\Longrightarrow \sqrt{\bar{\alpha}_t} \mathbf{x}_0 = \mathbf{x}_t + (1 - \bar{\alpha}_t) \nabla_{\mathbf{x}_t} \log p(\mathbf{x}_t)$$

$$\Longrightarrow \sqrt{\bar{\alpha}_t} \mathbf{x}_0 - \mathbf{x}_t = (1 - \bar{\alpha}_t) \nabla_{\mathbf{x}_t} \log p(\mathbf{x}_t).$$
(20)

Reuse the reparameterized version of Eq. (2), with $\epsilon \sim \mathcal{N}(\mathbf{0}, \mathbf{I})$,

$$\mathbf{x}_{t} = \sqrt{\bar{\alpha}_{t}} \mathbf{x}_{0} + \sqrt{1 - \bar{\alpha}_{t}} \boldsymbol{\epsilon}$$

$$\implies \sqrt{\bar{\alpha}_{t}} \mathbf{x}_{0} - \mathbf{x}_{t} = -\sqrt{1 - \bar{\alpha}_{t}} \boldsymbol{\epsilon}.$$
(21)

Combining Eq. (20) and Eq. (21), we obtain

$$\nabla_{\mathbf{x}_t} \log p(\mathbf{x}_t) = -\frac{\epsilon}{\sqrt{1 - \bar{\alpha}_t}}.$$
 (22)

Corollary 2. The objective in Eq. (10) is extensive to \mathbf{x}_0 -prediction or \mathbf{v} -prediction [50] in diffusion.

Proof. We provide the proof for \mathbf{x}_0 -prediction and \mathbf{v} -prediction variants separately.

As a recall, the objective Eq. (10) is built on the estimation given by ϵ -prediction in Eq. (9).

For the sake of clarity, here we re-present the formula but neglect the estimation error:

$$\epsilon = \sum_{y} p(y \mid \mathbf{x}_t) \epsilon_{\phi}(\mathbf{x}_t, t, \mathbf{c}_y). \tag{23}$$

For \mathbf{x}_0 -prediction, we employ data predictor $\mathbf{x}_{\phi}(\mathbf{x}_t, t, \mathbf{c})$ to predict \mathbf{x}_0 .

As we have the formula $\mathbf{x}_t = \sqrt{\bar{\alpha}_t} \mathbf{x}_0 + \sqrt{1 - \bar{\alpha}_t} \epsilon$, it can be deduced that $\forall \mathbf{c} \in \{\mathbf{c}_y : y \in \mathcal{Y}\} \cup \{\varnothing\}$,

$$\mathbf{x}_{t} = \sqrt{\bar{\alpha}_{t}} \mathbf{x}_{\phi}(\mathbf{x}_{t}, t, \mathbf{c}) + \sqrt{1 - \bar{\alpha}_{t}} \boldsymbol{\epsilon}_{\phi}(\mathbf{x}_{t}, t, \mathbf{c}). \tag{24}$$

Thus we have

$$\mathbf{x}_{0} = \frac{\mathbf{x}_{t} - \sqrt{1 - \bar{\alpha}_{t}} \boldsymbol{\epsilon}}{\sqrt{\bar{\alpha}_{t}}}$$

$$= \frac{\mathbf{x}_{t} - \sqrt{1 - \bar{\alpha}_{t}} \sum_{y} p(y \mid \mathbf{x}_{t}) \boldsymbol{\epsilon}_{\phi}(\mathbf{x}_{t}, t, \mathbf{c}_{y})}{\sqrt{\bar{\alpha}_{t}}} \qquad (Eq. (23))$$

$$= \frac{\sum_{y} p(y \mid \mathbf{x}_{t}) \left(\mathbf{x}_{t} - \sqrt{1 - \bar{\alpha}_{t}} \boldsymbol{\epsilon}_{\phi}(\mathbf{x}_{t}, t, \mathbf{c}_{y})\right)}{\sqrt{\bar{\alpha}_{t}}} \qquad \left(\sum_{y} p(y \mid \mathbf{x}_{t}) = 1\right)$$

$$= \frac{\sum_{y} p(y \mid \mathbf{x}_{t}) \sqrt{\bar{\alpha}_{t}} \mathbf{x}_{\phi}(\mathbf{x}_{t}, t, \mathbf{c}_{y})}{\sqrt{\bar{\alpha}_{t}}} \qquad (Eq. (24))$$

$$= \sum_{y} p(y \mid \mathbf{x}_{t}) \mathbf{x}_{\phi}(\mathbf{x}_{t}, t, \mathbf{c}_{y}).$$

Therefore objective in Eq. (10) can be rewritten as

$$\mathcal{L}_{DUSA}(\theta, \phi) = \mathbb{E}_{\epsilon} \left[\|\mathbf{x}_0 - \sum_{y} p_{\theta}(y \mid \mathbf{x}_0) \mathbf{x}_{\phi}(\mathbf{x}_t, t, \mathbf{c}_y) \|_2^2 \right].$$
 (26)

For v-prediction, we employ velocity predictor $\mathbf{v}_{\phi}(\mathbf{x}_t, t, \mathbf{c})$ to predict a constructed velocity objective

$$\mathbf{v}_t = \sqrt{\bar{\alpha}_t} \boldsymbol{\epsilon} - \sqrt{1 - \bar{\alpha}_t} \mathbf{x}_0. \tag{27}$$

Similar to the treatment above in Eq. (24), we have $\forall \mathbf{c} \in \{\mathbf{c}_y : y \in \mathcal{Y}\} \cup \{\emptyset\}$,

$$\mathbf{v}_{\phi}(\mathbf{x}_{t}, t, \mathbf{c}) = \sqrt{\bar{\alpha}_{t}} \boldsymbol{\epsilon}_{\phi}(\mathbf{x}_{t}, t, \mathbf{c}) - \sqrt{1 - \bar{\alpha}_{t}} \mathbf{x}_{\phi}(\mathbf{x}_{t}, t, \mathbf{c}). \tag{28}$$

Applying the conclusions in Eq. (23), Eq. (25) and Eq. (28), we have

$$\mathbf{v}_{t} = \sqrt{\bar{\alpha}_{t}} \boldsymbol{\epsilon} - \sqrt{1 - \bar{\alpha}_{t}} \mathbf{x}_{0}$$

$$= \sqrt{\bar{\alpha}_{t}} \sum_{y} p(y \mid \mathbf{x}_{t}) \boldsymbol{\epsilon}_{\phi}(\mathbf{x}_{t}, t, \mathbf{c}_{y}) - \sqrt{1 - \bar{\alpha}_{t}} \sum_{y} p(y \mid \mathbf{x}_{t}) \mathbf{x}_{\phi}(\mathbf{x}_{t}, t, \mathbf{c}_{y})$$

$$= \sum_{y} p(y \mid \mathbf{x}_{t}) \left(\sqrt{\bar{\alpha}_{t}} \boldsymbol{\epsilon}_{\phi}(\mathbf{x}_{t}, t, \mathbf{c}_{y}) - \sqrt{1 - \bar{\alpha}_{t}} \mathbf{x}_{\phi}(\mathbf{x}_{t}, t, \mathbf{c}_{y}) \right)$$

$$= \sum_{y} p(y \mid \mathbf{x}_{t}) \mathbf{v}_{\phi}(\mathbf{x}_{t}, t, \mathbf{c}_{y}).$$
(29)

Therefore, objective in Eq. (10) can be rewritten as

$$\mathcal{L}_{DUSA}(\theta, \phi) = \mathbb{E}_{\epsilon} \left[\| \mathbf{v}_t - \sum_{y} p_{\theta}(y \mid \mathbf{x}_0) \mathbf{v}_{\phi}(\mathbf{x}_t, t, \mathbf{c}_y) \|_2^2 \right].$$
(30)

D On the Estimation Bias and Efficiency of Diffusion-TTA and DUSA

D.1 Diffusion-TTA

Prior works [25, 29, 30, 32] rely on the Monte Carlo method for a good estimation of the likelihood.

The core of diffusion model formulation is the evidence lower bound (ELBO), also called variational lower bound (VLB), where the log-likelihood of data is bounded:

$$\log p_{\phi}(\mathbf{x}_0 \mid \mathbf{c}) \ge \mathbb{E}_q \left[\log \frac{p_{\phi}(\mathbf{x}_{0:T} \mid \mathbf{c})}{q(\mathbf{x}_{1:T} \mid \mathbf{x}_0)} \right], \tag{31}$$

where q is the forward (diffusion) process, and $p_{\phi}(\cdot)$ is the reverse process modeled by diffusion models parameterized by ϕ .

https://doi.org/10.52202/079017-0389

The ELBO can be further deduced and simplified with diffusion loss, we have

$$\mathbb{E}_{q} \left[\log \frac{p_{\phi}(\mathbf{x}_{0:T} \mid \mathbf{c})}{q(\mathbf{x}_{1:T} \mid \mathbf{x}_{0})} \right] \\
= \mathbb{E}_{q} \log p_{\phi}(\mathbf{x}_{0} \mid \mathbf{x}_{1}, \mathbf{c}) - \sum_{t=2}^{T} \mathbb{E}_{q} D_{KL}(q(\mathbf{x}_{t-1} \mid \mathbf{x}_{t}, \mathbf{x}_{0}) \parallel p_{\phi}(\mathbf{x}_{t-1} \mid \mathbf{x}_{t}, \mathbf{c})) \\
- D_{KL}(q(\mathbf{x}_{T} \mid \mathbf{x}_{0}) \parallel p_{\phi}(\mathbf{x}_{T})) \\
= -\mathbb{E}_{\boldsymbol{\epsilon}, t} \left[\sum_{t=2}^{T} w_{t} \|\boldsymbol{\epsilon} - \boldsymbol{\epsilon}_{\phi}(\mathbf{x}_{t}, t, \mathbf{c})\|_{2}^{2} - \log p_{\phi}(\mathbf{x}_{0} \mid \mathbf{x}_{1}, \mathbf{c}) \right] + C \\
\approx -T \mathbb{E}_{\boldsymbol{\epsilon}, t} \left[\|\boldsymbol{\epsilon} - \boldsymbol{\epsilon}_{\phi}(\mathbf{x}_{t}, t, \mathbf{c})\|_{2}^{2} \right] + C. \quad (\log p_{\phi}(\mathbf{x}_{0} \mid \mathbf{x}_{1}, \mathbf{c}) \text{ typically small, } w_{t} \leftarrow 1)$$
(32)

In the equations above, a theoretical approximation is made by simplifying weights w_t to 1 and ignoring the $\log p_{\phi}(\mathbf{x}_0 \mid \mathbf{x}_1, \mathbf{c})$ term. This simplification introduces **theoretical bias** relative to the true likelihood, as the approximation in Eq. (32) prevents the equality in Eq. (31) from holding.

Therefore, with a uniform prior on label space, the objective of Diffusion-TTA [32] is

$$\max_{y} p(y \mid \mathbf{x}) = \max_{y} p(\mathbf{x} \mid y) p(y) \qquad (\text{Bayes theorem})$$

$$= \max_{y} p(\mathbf{x} \mid y) \qquad (\text{uniform prior})$$

$$\gtrsim \max_{y} \exp\left(-T\mathbb{E}_{t,\epsilon} \left[\|\boldsymbol{\epsilon} - \boldsymbol{\epsilon}_{\phi}(\mathbf{x}_{t}, t, \mathbf{c}_{y})\|_{2}^{2}\right] + C\right) \qquad (\text{Eq. (32)})$$

$$= \min_{y} \mathbb{E}_{t,\epsilon} \left[\|\boldsymbol{\epsilon} - \boldsymbol{\epsilon}_{\phi}(\mathbf{x}_{t}, t, \mathbf{c}_{y})\|_{2}^{2}\right].$$
(33)

The objective thus takes expectation over ϵ and t, where Diffusion-TTA finds t plays a crucial rule in the final result and applies Monte Carlo method on 180 samples of t, for every single data sample.

D.2 DUSA

In contrast, our DUSA approach does not rely on the ELBO for likelihood maximization. Instead, we leverage the structured semantic priors introduced in Eq. (4) to guide the task model in extracting knowledge from the diffusion model using a single timestep. Notably, the only estimations in our method are the noise predictions $\epsilon \approx \epsilon_{\phi}(\mathbf{x}_t, t, \mathbf{c}_y)$ in Eq. (8), which are provably unbiased.

To elaborate, the diffusion models are typically optimized with the following simplified objective:

$$\mathcal{L}_{simple}(\phi) = \mathbb{E}_{\mathbf{x}_t | \boldsymbol{\epsilon}, t} [\| \boldsymbol{\epsilon} - \boldsymbol{\epsilon}_{\phi}(\mathbf{x}_t, t, \mathbf{c}_y) \|_2^2]. \tag{34}$$

At its optimal point, the noise estimations should satisfy:

$$\frac{\partial \mathcal{L}_{simple}(\phi)}{\partial \epsilon_{\phi}} = \mathbb{E}_{\mathbf{x}_{t} | \epsilon, t}[2(\epsilon - \epsilon_{\phi}(\mathbf{x}_{t}, t, \mathbf{c}_{y}))] = 0, \tag{35}$$

which implies the following:

$$\mathbb{E}_{\mathbf{x}_t|\boldsymbol{\epsilon},t}[\boldsymbol{\epsilon}_{\phi}(\mathbf{x}_t,t,\mathbf{c}_y)] = \mathbb{E}_{\mathbf{x}_t|\boldsymbol{\epsilon},t}[\boldsymbol{\epsilon}] = \boldsymbol{\epsilon}.$$
 (36)

Therefore, the conditional noise estimation ϵ_{ϕ} is an **unbiased estimator** of the true noise ϵ :

$$\operatorname{Bias}(\boldsymbol{\epsilon}_{\phi}(\mathbf{x}_{t}, t, \mathbf{c}_{y}), \boldsymbol{\epsilon}) = \mathbb{E}_{\mathbf{x}_{t} \mid \boldsymbol{\epsilon} t}[\boldsymbol{\epsilon}_{\phi}(\mathbf{x}_{t}, t, \mathbf{c}_{y})] - \boldsymbol{\epsilon} = 0. \tag{37}$$

Similarly, the unconditional noise estimation $\epsilon \approx \epsilon_{\phi}(\mathbf{x}_t, t, \emptyset)$ in Eq. (11) is also provably unbiased.

E Algorithm of DUSA

Algorithm 1: DiffUsion Score for test-time Adaptation (DUSA)

- 1: **Input:** Test samples $\{\mathbf{x}_0^j\}_{j=1}^M$, discriminative task model f_θ , generative diffusion model ϵ_ϕ , timestep t, learning rate η .
- 2: **Output:** Task predictions $\{\hat{y}_i\}_{i=1}^M$.
- 3: **for** j = 1 to M **do**
- 4: Predict logits $\mathbf{z} = f_{\theta}(\mathbf{x}_0^j)$ with task model.
- 5: Make task prediction $\hat{y}_j = \operatorname{argmax}_y \mathbf{z}_y$.
- 6: Apply CSM to prune logits \mathbf{z} to K classes and get $\hat{\mathbf{z}}$.
- 7: Take softmax over $\hat{\mathbf{z}}$ to get probabilities $\{p_{\theta}(y \mid \mathbf{x}_0^j)\}_{u=1}^K$.
- 8: Compute conditions $\{\mathbf{c}_y\}_{y=1}^K$ for all classes in $\hat{\mathbf{z}}$.
- 9: Sample noise ϵ and get noisy sample \mathbf{x}_t^j as in Eq. (2).
- 10: Get conditional noise predictions $\{\epsilon_{\phi}(\mathbf{x}_t^j, t, \mathbf{c}_y)\}_{y=1}^K$.
- 11: Calculate the objective $\mathcal{L}(\theta, \phi)$ in Eq. (10) or Eq. (13).
- 12: Update task model weights $\theta \leftarrow \theta \eta \nabla_{\theta} \mathcal{L}(\theta, \hat{\phi})$.
- 13: Update diffusion model weights $\phi \leftarrow \phi \eta \nabla_{\phi} \mathcal{L}(\theta, \phi)$.
- 14: **end for**

F More Experimental Details

F.1 More Details on Datasets

ImageNet-C [31]. ImageNet-C consists of corrupted images computed from applying algorithmic corruptions to the ImageNet [65] validation set, which has 50,000 images. To construct ImageNet-C, 15 corruptions that fall into 4 categories are applied separately to the whole validation set, including Gaussian noise (Gauss.), shot noise (Shot), impulse noise (Impl.), defocus blur (Defoc.), glass blur (Glass), motion blur (Motion), zoom blur (Zoom), snow (Snow), frost (Frost), fog (Fog), brightness (Brit.), contrast (Contr.), elastic transformation (Elastic), pixelation (Pixel) and JPEG compression (JPEG). Each corruption type has 5 severity levels and a higher severity level means a more severe distribution shift. We use the highest severity level 5 in all our experiments.

ADE20K [56]. ADE20K is a semantic segmentation dataset containing more than 20k images annotated with pixel-level labels on instances and object parts, among which 2k images are for validation. A total of 150 semantic classes are benchmarked for evaluation. We apply the corruptions defined in [31] with tools provided by [105] to construct ADE20K-C, which shares the corruption types with ImageNet-C, at the highest severity level 5. We use this corrupted benchmark for test-time semantic segmentation tasks.

F.2 More Details on Compared Methods

BN Adapt [62, 63, 66]. BN Adapt has the straightforward idea that the statistics in Batch Normalization layers are data-dependent, and therefore can be adapted at test time for better generalization.

Tent [44]. Tent is a pioneer in addressing the fully test-time adaptation problem. In the work, test-time batch normalization is employed to recalibrate the statistics within Batch Normalization, where features are normalized based on the current batch's statistics. Additionally, Tent utilizes entropy minimization to adjust the affine parameters of Batch Normalization layers.

CoTTA [45]. CoTTA focuses on performing test-time adaptation for continually changing distributions. Firstly, it generates more robust and reliable pseudo labels through multiple data augmentations and employs a mean-teacher architecture to reduce error accumulation. Secondly, to prevent catastrophic forgetting, a stochastic restoration strategy is proposed, which randomly rolls back a portion of the student model's parameters. Meanwhile, in the mean-teacher architecture, all the parameters of the student model remain trainable.

EATA [60]. EATA is devoted to improving efficiency and preventing knowledge forgetting. Concretely, the unreliable and redundant test samples are filtered out by the value of prediction entropy and similarity to the mean prediction. Besides, an anti-forgetting regularization based on fisher importance is proposed. Additionally, only affine parameters in batch normalization layers are adapted.

SAR [59]. SAR points out the unreliability of entropy minimization and the instability of Batch Normalization layers during test-time adaptation. Motivated by this, it proposes a sharpness-aware and reliable entropy minimization for Group/Layer Normalization-based models. For time efficiency, only affine parameters in Group/Layer Normalization layers are optimized.

RoTTA [61]. RoTTA is dedicated to conducting test-time adaptation on complex test streams characterized by continually changing data distributions and temporally correlated label distributions. To begin with, it develops a prediction-balanced sampling strategy grounded in uncertainty and timeliness, ensuring the maintenance of a robust snapshot of the test distribution for adaptation. Furthermore, a robust batch normalization layer is devised to recalibrate normalization statistics by applying exponential moving averages to selected samples. Lastly, it introduces a timeliness reweighting strategy to attain stable and robust adaptation. Only affine parameters in robust batch normalization layers undergo training.

Diffusion-TTA [32]. Diffusion-TTA is proposed to adapt pre-trained task models using feedback from pre-trained diffusion models. The integration of the task model into the diffusion model is achieved by modulating the conditioning of the diffusion model using the output of the task model. With the generative objective of diffusion models, the knowledge is backpropagated through conditioning to the task model. Hundreds of timesteps are sampled in a diffusion model for a single sample as an approximation of the likelihood estimation to improve adaptation performance.

F.3 More Details on Implementation

All pre-trained models involved in our paper are publicly available, including ResNet-50 (GN)², ViT-B/16 (LN)³, ConvNext-L (LN)⁴, DiT-XL/2⁵ and ControlNet⁶ based on Stable Diffusion v1.5⁷ from timm [106] or their official repository. The classifiers and DiT-XL/2 are pre-trained on ImageNet, while ADE20K is used to pre-train SegFormer-B5 and ControlNet.

As for code, we (re)implement all test-time adaptation methods for classification under a framework modified from MMPreTrain [103], except for Diffusion-TTA we adopt its official implementation. For test-time semantic segmentation tasks, we (re)implement all methods under a framework modified from MMSegmentation [104].

All experiments performed are with a batch size of 64, except for part of the analysis in Fig. 4. Our DUSA is trained with a batch size of 8 and a gradient accumulation of 8 steps, to yield an effective batch size of 64. Limited by its implementations, Diffusion-TTA is run with a batch size of 1, and a gradient accumulation of 64 steps is applied, also crafting an effective batch size of 64. We follow [32] and use Adam [64] optimizer with a learning rate of 0.00001 (1.0×10^{-5}) and a weight decay of 0.0 for both our DUSA and Diffusion-TTA, which applies to all classifiers. As for other compared methods, we use Stochastic Gradient Descent (SGD) with momentum 0.9 and a learning rate of 0.00025 (2.5×10^{-4}) for ResNet-50, while a learning rate of 0.001 (1.0×10^{-3}) is used for ViT-B/16, in accordance with the literature [44, 59, 60] to obtain decent baseline results. For ConvNext-L, we use Adam with a learning rate of 0.0001 (1.0×10^{-5}) with a weight decay of 0.0 for all methods involved. The diffusion model for classification tasks is a Diffusion Transformer

 $^{^2} https://github.com/rwightman/pytorch-image-models/releases/download/v0.1-rsb-weights/resnet50_gn_a1h2-8fe6c4d0.pth$

³https://storage.googleapis.com/vit_models/augreg/B_16-i1k-300ep-lr_0.001-aug_strong2-wd_0.1-do_0.1-sd_0.1--imagenet2012-steps_20k-lr_0.01-res_224.npz

⁴https://dl.fbaipublicfiles.com/convnext/convnext_large_1k_224_ema.pth

⁵https://dl.fbaipublicfiles.com/DiT/models/DiT-XL-2-256x256.pt

 $^{^6} https://huggingface.co/lllyasviel/control_v11p_sd15_seg/blob/main/diffusion_pytorch_model.bin$

 $^{^7}$ https://huggingface.co/runwayml/stable-diffusion-v1-5/blob/main/v1-5-pruned.ckpt

DiT-XL/2 [22] trained on ImageNet [65] from scratch. For all classification tasks on ImageNet-C, we adopt the standard pipeline [31] and center crop images to 224×224 for task models. Our DUSA and Diffusion-TTA both use DiT-XL/2 with an input size of 256×256 as the diffusion model, therefore we resize the cropped 224×224 image to 256×256 before passing it to DiT-XL/2 as input. During adaptation, we freeze the VAE encoder and condition embedder of DiT, while training the denoising transformer which functions in a latent space of $32 \times 32 \times 4$. All parameters of the task models are adapted in DUSA, as is done in Diffusion-TTA and CoTTA.

For hyperparameters in DUSA, we set t=100, k=4 and m=2 for all classification tasks. For the sake of fair comparison and practical considerations in compute resources, we give Diffusion-TTA the same budget b=6, i.e., 6 timesteps in diffusion models are randomly sampled for the training of each image sample, which applies to all results reported on Diffusion-TTA, including those in Fig. 3 and Fig. 4. For both our DUSA and Diffusion-TTA that involve diffusion models, the noise ϵ added to input data is randomly sampled. As for other compared methods, we follow all hyperparameters in their original setup and please refer to their paper for more detailed hyperparameter settings.

For test-time semantic segmentation, we follow [45] and use a batch size of 1, Adam optimizer with a learning rate of 0.00006/8 ($6.0 \times 10^{-5}/8$) and a weight decay of 0.0 for all methods. The diffusion model for this task is a ControlNet [48] finetuned from Stable Diffusion v1.5 [20] on ADE20K. Note that ControlNets come with extra conditioning capability, but we dismiss extra conditions beyond text so that it can be recognized as a typical text-to-image diffusion model. In detail, the conditioning of our used ConvNeXt accepts a colored segmentation map as input, and there is a color rgb(0,0,0) for a background/undefined category, which is not among the 150 ADE20K classes, so we find it suitable to use all-zero colormaps as the conditioning and regard the ControlNet as only receiving meaningful conditions from texts. While adapting, we again freeze the VAE encoders and text embedder, while training the denoising UNet, along with the ControlNet branch plugged in. For the task model SegFormer-B5, the input size is 512×512 , so we resize the shorter side of input images to 512 while keeping the aspect ratio for all methods involved. As for our DUSA, the ControlNet requires an input size of 512×512 . To get the most of semantic priors from diffusion models, we apply a sliding strategy to both ControlNet input (which is a non-square input with a 512 short side) and SegFormer output, which aligns the task model forward with compared methods, and thus the sliding on one image is finished in two steps. Note that SegFormer-B5 has a $4\times$ downsample while ControlNet has a 8× downsample, therefore the logits of SegFormer-B5 can be larger than the latent space of ControlNet, so we further perform a 2× downsample on the logits to prepare for the aggregation of noise predictions in Eq. (14).

As we resort to the conventional **text-to-image** formulation of diffusion models, a whole noise estimation map is predicted each time a condition is given. This is much different from classification as the segmentation results are at the pixel level, making an image-level candidate class selection non-trivial. Note that LogitNorm is still present before selection, which is applied to the logits in the channel dimension. We make a little modification to the selection strategy here, instead of attempting to change the structure of diffusion models as done in [32], to prove the versatility of DUSA. Specifically, we allow a budget of 20 classes for each input image, which is also split into a task model-based top-1 selection budget and a random budget, inheriting the spirits of DUSA for classification. We first gather the unique set of top-1 predicted classes from all pixels. If the number of gathered classes already exceeds the budget, we randomly suppress the redundant classes. Otherwise, if there is a surplus in the budget, we further perform a random selection from the remaining classes until the threshold is reached. The subsequent steps are the same as in classification.

F.4 More Details on Compute Resources

We use Nvidia A6000 GPU with 48GB memory for all our experiments. For faster training, we use Automatic Mixed Precision with autocasts to fp16 for both classification and semantic segmentation. Additionally for semantic segmentation, gradient checkpointing is enabled for the task model. For test-time adaptation on classifiers with a batch size of 8, our DUSA takes around 43GB of memory and 1.5h training time for a single task (roughly 0.11s per image), while our DUSA-U takes around 28GB of memory and 1h training time for a single task (roughly 0.07s per image). For test-time semantic segmentation with a batch size of 1, we experiment on two Nvidia A6000 GPUs, with a total of 24GB+44GB=68GB and 2.5h training time for a single task (roughly 4.5s per image). As we perform three independent runs for each task, a total of 14 GPU days are required for results in

Table 1, 3 GPU days for Table 2, and 5 GPU days for Table 3, accumulating into around 22 A6000 GPU days for our main results. Preliminary experiments make the full research project require more compute than reported, but it's non-trivial for us to benchmark them all.

G Detailed Ablation Results on DUSA Components

We provide the detailed results in Table 4 for ResNet-50 and ConvNeXt-L on the three variants of corruptions in the Noise category in Table 5, namely Gaussian noise, Shot noise and Impulse noise, along with Pixelate corruption in the Digital category for ConvNeXt-L.

Table 5: Ablation on critical components in DUSA. Components in colored rows are not carried over to subsequent rows. Task-level results are provided for the Noise category.

					ResNet-50 (GN)			ConvNeXt-L (LN)			
Variants	k	m	D.F.	D.B.	Gauss.	Shot	Impul.	Gauss.	Shot	Impul.	Pixel
Source-only	0	0	0	0	22.1	23.0	22.0	56.7	56.2	58.3	42.3
+ score priors inspired loss (4)	4	0	4	0	23.5	26.7	27.8	31.1	48.1	53.1	9.2
+ LogitNorm (4)	4	0	4	0	42.5	45.3	44.2	59.3	61.7	61.7	9.6
+ adapt diffusion (4)	4	0	4	4	40.5	42.4	40.8	59.0	59.1	55.4	49.3
+ LogitNorm (4)	4	0	4	4	45.4	47.4	46.3	64.0	65.5	65.5	70.4
+ LogitNorm (6)	6	0	6	6	45.4	47.6	46.5	64.0	65.6	65.6	70.7
+ uniform select (6)	4	2	6	6	45.0	47.3	46.1	64.2	65.7	65.4	70.7
+ multinomial select (6) (DUSA)	4	2	6	6	45.2	47.3	46.4	64.2	65.6	65.5	70.8
+ null conditioning (6) (DUSA-U)	4	2	7	1	45.1	47.2	46.1	63.7	65.3	65.1	70.5

H Ensembling Timesteps in DUSA

In DUSA, we formulate our approach to extract knowledge from a single timestep, thereby enhancing the efficiency of adaptation. However, it is intriguing to investigate whether an ensemble of multiple timesteps would further improve performance. We experiment on ConvNeXt-L and present our findings in Table 6. The results indicate that, while ensembling timesteps does provide benefits, the performance gains may not be substantial enough to justify the increased computational overhead.

Table 6: Effects of ensembling timesteps in our DUSA. Experiments were conducted across four typical scenarios that fall into four main categories in ImageNet-C.

Timestep(s)	Gauss.	Defoc.	Snow	Contr.
{50}	64.0	50.8	69.5	69.3
{100}	64.2	54.7	70.1	68.9
{200}	63.4	55.1	69.8	66.6
{50,100}	64.3	54.0	70.2	69.2
{50,100,200}	64.3	55.4	70.2	69.1

I Visualization of Test-time Semantic Segmentation Results

We visualize the test-time semantic segmentation results of our DUSA and compared methods in Fig. 5. A model checkpoint is saved after test-time adaptation over a whole corrupted ADE20K validation set. The checkpoint is then used to yield segmentation maps. We show results from four main categories of corruption, and segmentation maps are colorized with the ADE20K palette for better visual effects. Our DUSA, which exploits the structured semantic priors underneath the score-based diffusion model, shows superior capability in correcting erroneous predictions and providing fine-grained segmentation results.

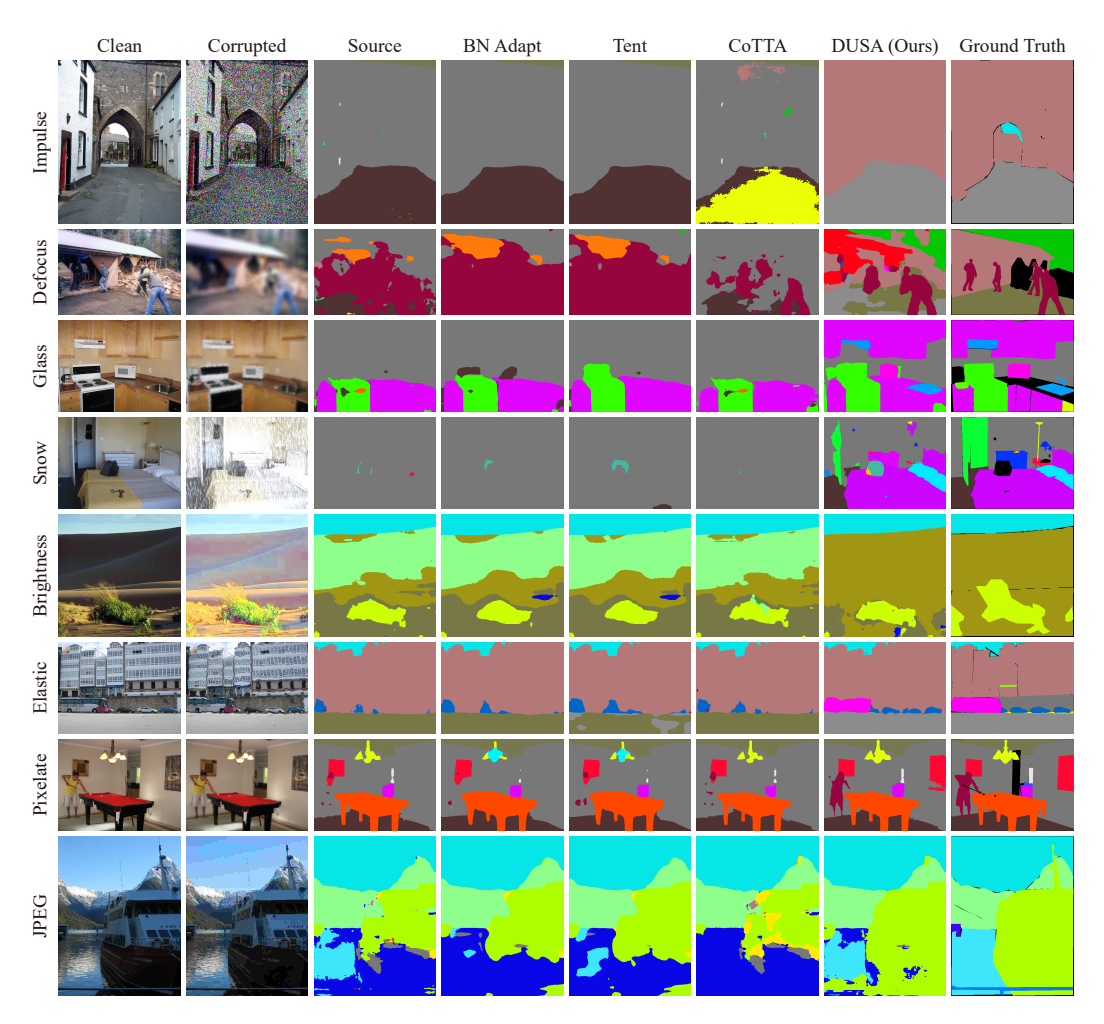


Figure 5: Visualization of test-time semantic segmentation results on ADE20K-C. From left to right: clean image from ADE20K, corrupted version of the image, results from source model, BN Adapt, Tent, CoTTA, our DUSA, and lastly the ground truth. DUSA results exhibit a favorable visual effect.

NeurIPS Paper Checklist

1. Claims

Question: Do the main claims made in the abstract and introduction accurately reflect the paper's contributions and scope?

Answer: [Yes]

Justification: We have clearly stated the contributions made in the paper and the scope both in the abstract and introduction.

Guidelines:

- The answer NA means that the abstract and introduction do not include the claims made in the paper.
- The abstract and/or introduction should clearly state the claims made, including the contributions made in the paper and important assumptions and limitations. A No or NA answer to this question will not be perceived well by the reviewers.
- The claims made should match theoretical and experimental results, and reflect how much the results can be expected to generalize to other settings.
- It is fine to include aspirational goals as motivation as long as it is clear that these goals are not attained by the paper.

2. Limitations

Question: Does the paper discuss the limitations of the work performed by the authors?

Answer: [Yes]

Justification: We have discussed the limitation of our work in Appendix A.

Guidelines:

- The answer NA means that the paper has no limitation while the answer No means that the paper has limitations, but those are not discussed in the paper.
- The authors are encouraged to create a separate "Limitations" section in their paper.
- The paper should point out any strong assumptions and how robust the results are to violations of these assumptions (e.g., independence assumptions, noiseless settings, model well-specification, asymptotic approximations only holding locally). The authors should reflect on how these assumptions might be violated in practice and what the implications would be.
- The authors should reflect on the scope of the claims made, e.g., if the approach was only tested on a few datasets or with a few runs. In general, empirical results often depend on implicit assumptions, which should be articulated.
- The authors should reflect on the factors that influence the performance of the approach. For example, a facial recognition algorithm may perform poorly when image resolution is low or images are taken in low lighting. Or a speech-to-text system might not be used reliably to provide closed captions for online lectures because it fails to handle technical jargon.
- The authors should discuss the computational efficiency of the proposed algorithms and how they scale with dataset size.
- If applicable, the authors should discuss possible limitations of their approach to address problems of privacy and fairness.
- While the authors might fear that complete honesty about limitations might be used by reviewers as grounds for rejection, a worse outcome might be that reviewers discover limitations that aren't acknowledged in the paper. The authors should use their best judgment and recognize that individual actions in favor of transparency play an important role in developing norms that preserve the integrity of the community. Reviewers will be specifically instructed to not penalize honesty concerning limitations.

3. Theory Assumptions and Proofs

Question: For each theoretical result, does the paper provide the full set of assumptions and a complete (and correct) proof?

Answer: [Yes]

Justification: We state the assumptions made in all theoretical results and properly referenced the Lemmas involved. Formal proofs are provided in Appendix C.

Guidelines

- The answer NA means that the paper does not include theoretical results.
- All the theorems, formulas, and proofs in the paper should be numbered and cross-referenced.
- All assumptions should be clearly stated or referenced in the statement of any theorems.
- The proofs can either appear in the main paper or the supplemental material, but if they appear in the supplemental material, the authors are encouraged to provide a short proof sketch to provide intuition.
- Inversely, any informal proof provided in the core of the paper should be complemented by formal proofs provided in appendix or supplemental material.
- Theorems and Lemmas that the proof relies upon should be properly referenced.

4. Experimental Result Reproducibility

Question: Does the paper fully disclose all the information needed to reproduce the main experimental results of the paper to the extent that it affects the main claims and/or conclusions of the paper (regardless of whether the code and data are provided or not)?

Answer: [Yes]

Justification: We have provided implementation details in Appendix F.3, the algorithm of our method in Appendix E, and attached code in the supplemental material.

Guidelines:

- The answer NA means that the paper does not include experiments.
- If the paper includes experiments, a No answer to this question will not be perceived
 well by the reviewers: Making the paper reproducible is important, regardless of
 whether the code and data are provided or not.
- If the contribution is a dataset and/or model, the authors should describe the steps taken to make their results reproducible or verifiable.
- Depending on the contribution, reproducibility can be accomplished in various ways. For example, if the contribution is a novel architecture, describing the architecture fully might suffice, or if the contribution is a specific model and empirical evaluation, it may be necessary to either make it possible for others to replicate the model with the same dataset, or provide access to the model. In general, releasing code and data is often one good way to accomplish this, but reproducibility can also be provided via detailed instructions for how to replicate the results, access to a hosted model (e.g., in the case of a large language model), releasing of a model checkpoint, or other means that are appropriate to the research performed.
- While NeurIPS does not require releasing code, the conference does require all submissions to provide some reasonable avenue for reproducibility, which may depend on the nature of the contribution. For example
 - (a) If the contribution is primarily a new algorithm, the paper should make it clear how to reproduce that algorithm.
- (b) If the contribution is primarily a new model architecture, the paper should describe the architecture clearly and fully.
- (c) If the contribution is a new model (e.g., a large language model), then there should either be a way to access this model for reproducing the results or a way to reproduce the model (e.g., with an open-source dataset or instructions for how to construct the dataset).
- (d) We recognize that reproducibility may be tricky in some cases, in which case authors are welcome to describe the particular way they provide for reproducibility. In the case of closed-source models, it may be that access to the model is limited in some way (e.g., to registered users), but it should be possible for other researchers to have some path to reproducing or verifying the results.

5. Open access to data and code

Question: Does the paper provide open access to the data and code, with sufficient instructions to faithfully reproduce the main experimental results, as described in supplemental material?

Answer: [Yes]

Justification: The datasets and pre-trained models used in our work are all from previous works and publicly available. We have provided dataset details in Appendix F.1, model weights URLs in Appendix F.3, and reproducible instructions with code attached in the supplemental material.

Guidelines:

- The answer NA means that paper does not include experiments requiring code.
- Please see the NeurIPS code and data submission guidelines (https://nips.cc/public/guides/CodeSubmissionPolicy) for more details.
- While we encourage the release of code and data, we understand that this might not be possible, so "No" is an acceptable answer. Papers cannot be rejected simply for not including code, unless this is central to the contribution (e.g., for a new open-source benchmark).
- The instructions should contain the exact command and environment needed to run to reproduce the results. See the NeurIPS code and data submission guidelines (https://nips.cc/public/guides/CodeSubmissionPolicy) for more details.
- The authors should provide instructions on data access and preparation, including how
 to access the raw data, preprocessed data, intermediate data, and generated data, etc.
- The authors should provide scripts to reproduce all experimental results for the new proposed method and baselines. If only a subset of experiments are reproducible, they should state which ones are omitted from the script and why.
- At submission time, to preserve anonymity, the authors should release anonymized versions (if applicable).
- Providing as much information as possible in supplemental material (appended to the paper) is recommended, but including URLs to data and code is permitted.

6. Experimental Setting/Details

Question: Does the paper specify all the training and test details (e.g., data splits, hyper-parameters, how they were chosen, type of optimizer, etc.) necessary to understand the results?

Answer: [Yes]

Justification: A brief yet informative specification is provided in Sec. 4. For more details, we specify dataset usage details in Appendix F.1, models, optimizers and hyperparameters details in Appendix F.3.

Guidelines:

- The answer NA means that the paper does not include experiments.
- The experimental setting should be presented in the core of the paper to a level of detail that is necessary to appreciate the results and make sense of them.
- The full details can be provided either with the code, in appendix, or as supplemental material.

7. Experiment Statistical Significance

Question: Does the paper report error bars suitably and correctly defined or other appropriate information about the statistical significance of the experiments?

Answer: [Yes]

Justification: We report all our main results with mean & standard deviation, the results are obtained by independent running over three random seeds for each task.

Guidelines:

- The answer NA means that the paper does not include experiments.
- The authors should answer "Yes" if the results are accompanied by error bars, confidence intervals, or statistical significance tests, at least for the experiments that support the main claims of the paper.

- The factors of variability that the error bars are capturing should be clearly stated (for example, train/test split, initialization, random drawing of some parameter, or overall run with given experimental conditions).
- The method for calculating the error bars should be explained (closed form formula, call to a library function, bootstrap, etc.)
- The assumptions made should be given (e.g., Normally distributed errors).
- It should be clear whether the error bar is the standard deviation or the standard error of the mean.
- It is OK to report 1-sigma error bars, but one should state it. The authors should preferably report a 2-sigma error bar than state that they have a 96% CI, if the hypothesis of Normality of errors is not verified.
- For asymmetric distributions, the authors should be careful not to show in tables or figures symmetric error bars that would yield results that are out of range (e.g. negative error rates).
- If error bars are reported in tables or plots, The authors should explain in the text how they were calculated and reference the corresponding figures or tables in the text.

8. Experiments Compute Resources

Question: For each experiment, does the paper provide sufficient information on the computer resources (type of compute workers, memory, time of execution) needed to reproduce the experiments?

Answer: [Yes]

Justification: The compute resource are provided in Appendix F.4.

Guidelines:

- The answer NA means that the paper does not include experiments.
- The paper should indicate the type of compute workers CPU or GPU, internal cluster, or cloud provider, including relevant memory and storage.
- The paper should provide the amount of compute required for each of the individual experimental runs as well as estimate the total compute.
- The paper should disclose whether the full research project required more compute than the experiments reported in the paper (e.g., preliminary or failed experiments that didn't make it into the paper).

9. Code Of Ethics

Question: Does the research conducted in the paper conform, in every respect, with the NeurIPS Code of Ethics https://neurips.cc/public/EthicsGuidelines?

Answer: [Yes]

Justification: We have preserved anonymity in all submitted materials.

Guidelines:

- The answer NA means that the authors have not reviewed the NeurIPS Code of Ethics.
- If the authors answer No, they should explain the special circumstances that require a deviation from the Code of Ethics.
- The authors should make sure to preserve anonymity (e.g., if there is a special consideration due to laws or regulations in their jurisdiction).

10. Broader Impacts

Question: Does the paper discuss both potential positive societal impacts and negative societal impacts of the work performed?

Answer: [Yes]

Justification: We have discussed the potential societal impacts in Appendix A.

Guidelines:

- The answer NA means that there is no societal impact of the work performed.
- If the authors answer NA or No, they should explain why their work has no societal impact or why the paper does not address societal impact.

- Examples of negative societal impacts include potential malicious or unintended uses (e.g., disinformation, generating fake profiles, surveillance), fairness considerations (e.g., deployment of technologies that could make decisions that unfairly impact specific groups), privacy considerations, and security considerations.
- The conference expects that many papers will be foundational research and not tied to particular applications, let alone deployments. However, if there is a direct path to any negative applications, the authors should point it out. For example, it is legitimate to point out that an improvement in the quality of generative models could be used to generate deepfakes for disinformation. On the other hand, it is not needed to point out that a generic algorithm for optimizing neural networks could enable people to train models that generate Deepfakes faster.
- The authors should consider possible harms that could arise when the technology is being used as intended and functioning correctly, harms that could arise when the technology is being used as intended but gives incorrect results, and harms following from (intentional or unintentional) misuse of the technology.
- If there are negative societal impacts, the authors could also discuss possible mitigation strategies (e.g., gated release of models, providing defenses in addition to attacks, mechanisms for monitoring misuse, mechanisms to monitor how a system learns from feedback over time, improving the efficiency and accessibility of ML).

11. Safeguards

Question: Does the paper describe safeguards that have been put in place for responsible release of data or models that have a high risk for misuse (e.g., pretrained language models, image generators, or scraped datasets)?

Answer: [NA]

Justification: The datasets and models used in the paper are all publicly available and from previous works.

Guidelines:

- The answer NA means that the paper poses no such risks.
- Released models that have a high risk for misuse or dual-use should be released with
 necessary safeguards to allow for controlled use of the model, for example by requiring
 that users adhere to usage guidelines or restrictions to access the model or implementing
 safety filters.
- Datasets that have been scraped from the Internet could pose safety risks. The authors should describe how they avoided releasing unsafe images.
- We recognize that providing effective safeguards is challenging, and many papers do not require this, but we encourage authors to take this into account and make a best faith effort.

12. Licenses for existing assets

Question: Are the creators or original owners of assets (e.g., code, data, models), used in the paper, properly credited and are the license and terms of use explicitly mentioned and properly respected?

Answer: [Yes]

Justification: The datasets, models and code used in the paper are from previous works and are publicly available. We have cited related papers, respect their license, and include their license in Appendix B.

Guidelines:

- The answer NA means that the paper does not use existing assets.
- The authors should cite the original paper that produced the code package or dataset.
- The authors should state which version of the asset is used and, if possible, include a URL.
- The name of the license (e.g., CC-BY 4.0) should be included for each asset.
- For scraped data from a particular source (e.g., website), the copyright and terms of service of that source should be provided.

- If assets are released, the license, copyright information, and terms of use in the
 package should be provided. For popular datasets, paperswithcode.com/datasets
 has curated licenses for some datasets. Their licensing guide can help determine the
 license of a dataset.
- For existing datasets that are re-packaged, both the original license and the license of the derived asset (if it has changed) should be provided.
- If this information is not available online, the authors are encouraged to reach out to the asset's creators.

13. New Assets

Question: Are new assets introduced in the paper well documented and is the documentation provided alongside the assets?

Answer: [NA]

Justification: No new assets are released in our work.

Guidelines:

- The answer NA means that the paper does not release new assets.
- Researchers should communicate the details of the dataset/code/model as part of their submissions via structured templates. This includes details about training, license, limitations, etc.
- The paper should discuss whether and how consent was obtained from people whose asset is used.
- At submission time, remember to anonymize your assets (if applicable). You can either create an anonymized URL or include an anonymized zip file.

14. Crowdsourcing and Research with Human Subjects

Question: For crowdsourcing experiments and research with human subjects, does the paper include the full text of instructions given to participants and screenshots, if applicable, as well as details about compensation (if any)?

Answer: [NA]

Justification: This paper does not involve crowdsourcing nor research with human subjects.

Guidelines:

- The answer NA means that the paper does not involve crowdsourcing nor research with human subjects.
- Including this information in the supplemental material is fine, but if the main contribution of the paper involves human subjects, then as much detail as possible should be included in the main paper.
- According to the NeurIPS Code of Ethics, workers involved in data collection, curation, or other labor should be paid at least the minimum wage in the country of the data collector.

15. Institutional Review Board (IRB) Approvals or Equivalent for Research with Human Subjects

Question: Does the paper describe potential risks incurred by study participants, whether such risks were disclosed to the subjects, and whether Institutional Review Board (IRB) approvals (or an equivalent approval/review based on the requirements of your country or institution) were obtained?

Answer: [NA]

Justification: This paper does not involve crowdsourcing nor research with human subjects. Guidelines:

- The answer NA means that the paper does not involve crowdsourcing nor research with human subjects.
- Depending on the country in which research is conducted, IRB approval (or equivalent) may be required for any human subjects research. If you obtained IRB approval, you should clearly state this in the paper.

- We recognize that the procedures for this may vary significantly between institutions and locations, and we expect authors to adhere to the NeurIPS Code of Ethics and the guidelines for their institution.
- For initial submissions, do not include any information that would break anonymity (if applicable), such as the institution conducting the review.